Integrated view and comparative analysis of baseline protein expression in mouse and rat tissues

Shengbo Wang[1†], David García-Seisdedos[1,2†], Ananth Prakash[1,2†*], Deepti Jaiswal Kundu[1], Andrew Collins[3], Nancy George[1], Silvie Fexova[1], Pablo Moreno[1], Irene Papatheodorou[1,2], Andrew R. Jones[3], Juan Antonio Vizcaíno[1,2 *]

[1] European Molecular Biology Laboratory - European Bioinformatics Institute (EMBL-EBI), Wellcome Genome Campus, Hinxton, Cambridge, CB10 1SD. United Kingdom.

[2] Open Targets, Wellcome Genome Campus, Hinxton, Cambridge, CB10 1SD. United Kingdom.

[3] Institute of Systems, Molecular and Integrative Biology, University of Liverpool, Liverpool L69 7ZB, United Kingdom.

*Corresponding authors.

†All three authors have contributed equally and they wish to be considered as joint first authors.

Dr. Ananth Prakash. European Molecular Biology Laboratory, European Bioinformatics Institute (EMBL-EBI), Wellcome Trust Genome Campus, Hinxton, Cambridge, CB10 1SD, UK. Phone: + 44 (0) 1223 492610. Email: ananth@ebi.ac.uk

Dr. Juan Antonio Vizcaíno. European Molecular Biology Laboratory, European Bioinformatics Institute (EMBL-EBI), Wellcome Trust Genome Campus, Hinxton, Cambridge, CB10 1SD, UK. Phone: + 44 (0) 1223 492686. Email: juan@ebi.ac.uk.

Keywords

Mass spectrometry, quantitative proteomics, comparative protein expression, public data reuse, rat proteome, mouse proteome, PRIDE database

Abstract

The increasingly large amount of proteomics data in the public domain enables, among other applications, the combined analyses of datasets to create comparative protein expression maps covering different organisms and different biological conditions. Here we have reanalysed public proteomics datasets from mouse and rat tissues (14 and 9 datasets, respectively), to assess baseline protein abundance. Overall, the aggregated dataset contained 23 individual datasets, including a total of 211 samples coming from 34 different tissues across 14 organs, comprising 9 mouse and 3 rat strains, respectively.

In all cases, we studied the distribution of canonical proteins between the different organs. The number of canonical proteins per dataset ranged from 273 (tendon) and 9,715 (liver) in mouse, and from 101 (tendon) and 6,130 (kidney) in rat. Then, we studied how protein abundances compared across different datasets and organs for both species. As a key point we carried out a comparative analysis of protein expression between mouse, rat and human tissues. We observed a high level of correlation of protein expression among orthologs between all three species in brain, kidney, heart and liver samples, whereas the correlation of protein expression was generally slightly lower between organs within the same species. Protein expression results have been integrated into the resource Expression Atlas for widespread dissemination.

Author summary

We have reanalysed 23 baseline mass spectrometry-based public proteomics datasets stored in the PRIDE database. Overall, the aggregated dataset contained 211 samples, coming from 34 different tissues across 14 organs, comprising 9 mouse and 3 rat strains, respectively. We analysed the distribution of protein expression across organs in both species. We also studied how protein abundances compared across different datasets and organs for both species. Then we performed gene ontology and pathway enrichment analyses to identify enriched biological processes and pathways across organs. We also carried out a comparative analysis of baseline protein expression across mouse, rat and human tissues, observing a high level of expression correlation among orthologs in all three species, in brain, kidney, heart and liver samples. To disseminate these findings, we have integrated the protein expression results into the resource Expression Atlas.

1. Introduction

High-throughput mass spectrometry (MS)-based proteomics approaches have matured significantly in recent years, becoming an essential tool in biological research [1]. This has been the consequence of very significant technical improvements in MS instrumentation, chromatography, automation in sample preparation and computational analyses, among other areas. The most used MS-based experimental approach is Data Dependent Acquisition (DDA) bottom-up proteomics. Among the main quantitative proteomics DDA techniques, label-free intensity-based approaches remain very popular, although labelled-approaches, especially those techniques based on the isotopic labelling of peptides (MS^2 labelling), such as iTRAQ (Isobaric tag for relative and absolute quantitation) and TMT (Tandem Mass Tagging), are becoming increasingly used as well.

Following the steps initiated by genomics and transcriptomics, open data practices in the field have become embedded and commonplace in proteomics in recent years. In this context, datasets are now commonly available in the public domain to support the claims published in the corresponding manuscripts. The PRIDE database [2], located at the European Bioinformatics Institute (EBI), is currently the largest resource worldwide for public proteomics data deposition. PRIDE is also one of the founding members of the global ProteomeXchange consortium [3], involving five other resources, namely PeptideAtlas, MassIVE, iProX, jPOST and PanoramaPublic. ProteomeXchange has standardised data submission and dissemination of public proteomics data worldwide.

As a consequence, there is an unprecedented availability of data in the public domain, which is triggering multiple applications [4], including the joint reanalysis of datasets (so-called

94 meta-analysis studies) [5-7]. Indeed, public proteomics datasets can be systematically
95 reanalysed and integrated e.g., to confirm the results reported in the original publications,
96 potentially in a more robust manner since evidence can be strengthened if it is found
97 consistently across different datasets. Potentially, new insights different to the aims of the
98 original studies can also be obtained by reanalysing the datasets using different strategies, this
99 includes repurposing of public datasets [8], including for instance approaches such as
100 proteogenomics studies for genome annotation purposes [9-12].
101
102 In this context of reuse of public proteomics data, PRIDE has started to work on developing
103 data dissemination and integration pipelines into popular added-value resources at the EBI.
104 This is perceived as a more sustainable approach in the medium-long term than setting up
105 new independent bioinformatics resources. One of them is Expression Atlas [13], a resource
106 that has enabled over the years easy access to gene expression data across species, tissues,
107 cells, experimental conditions and diseases. Only recently, protein expression information
108 coming from reanalysed datasets has been integrated in the 'bulk' section of Expression
109 Atlas. As a result, proteomics expression data can be integrated with transcriptomics
110 information, mostly coming from RNA-Seq experiments. So far, we have performed two
111 meta-analysis studies involving the reanalysis and integration of: (i) 11 public quantitative
112 datasets coming from cell lines and human tumour samples [13]; and (ii) 24 human baseline
113 datasets coming from 31 different organs [14].
114
115 The next logical step is to perform an analogous study of baseline protein expression in two
116 of the main model organisms: *Mus musculus* and *Rattus norvegicus*. To date, there are only a
117 small number of bioinformatics resources providing access to reanalysed MS-based
118 quantitative proteomics datasets, and even fewer if one considers only mouse and rat data. In

119 this context, at the end of 2020, ProteomicsDB [15] released a first version of the mouse
120 proteome, based on the reanalysis of five label-free datasets. To the best of our knowledge,
121 there is no such public resource storing accurate MS-derived data for rat data yet. PaxDB is a
122 resource [16] that provides protein expression information coming from many species
123 (including mouse and rat) but the reported data relies on spectral counting, a technique that
124 generally does not provide the same level of accuracy than intensity-based label-free
125 approaches. Additionally, although antibody-based human protein expression information is
126 provided *via* the Human Protein Atlas [17] , their efforts are focused on human protein
127 expression.
128
129 Here, we report the reanalysis and integration of 23 public mouse (14 datasets) and rat (9
130 datasets) label-free datasets, and the incorporation of the results into the resource Expression
131 Atlas as baseline studies. Additionally, we report a comparative analysis of protein
132 expression across mouse, rat and human (in this case using the results reported at [14] using
133 the same methodology).
134

2. Results

2.1. Baseline proteomics datasets

Overall, we quantified protein expression from 34 healthy tissues in 14 organs coming from 23 datasets. The analyses covered a total of 1,173 MS runs from 211 samples that were annotated as healthy/control/non-treated samples, thus representing baseline protein expression. Non-control/disease samples associated with these datasets were also reanalysed but are not discussed here. Normalised protein abundances values (as ppb, parts per billion, see Methods for calculation) from both control/healthy/non-treated and disease/treated tissue samples are available to view as heatmaps in Expression Atlas. The protein abundances along with sample annotations, sample quality assessment summary and experimental parameter inputs for MaxQuant can be downloaded from Expression Atlas as text files. A summary of the data selection and reanalysis protocols is shown in Fig. 1. The total number of peptides and proteins identified in these datasets are shown in Table 1.

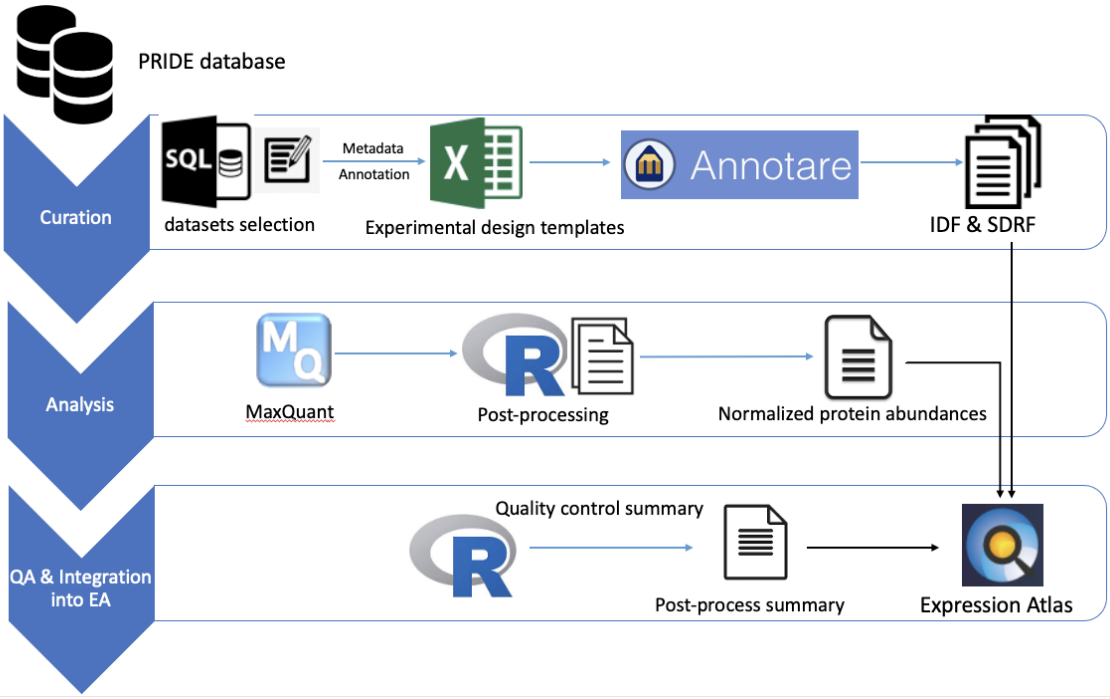

Figure 1. An overview of the study design and reanalysis pipeline. QA: Quality assessment.

Expression Atlas accession numbers	PRIDE dataset identifiers	Tissues	Organs	Species	Strains	Fractionation	Number of MS runs	Number of samples	Number of protein groups†	Number of peptides †	Number of unique peptides†	Number of unique genes mapped†
E-PROT-7§	PXD000867 [18]	Liver	Liver	*Mus musculus*	C57BL/6J	Yes	24	4	12,792	246,738	167,725	9,715
E-PROT-10§	PXD000288 [19]	Triceps muscles	Triceps Muscles	*Mus musculus*	C57BL/6	Yes	36	3	10,870	189,553	126,670	6,421
E-PROT-16	PXD003155 [20]	Cerebellum, Liver	Brain, Liver	*Mus musculus*	C57BL/6	No	24	12	4,508	59,696	45,728	3,797
E-PROT-74	PXD004612 [21]	Achilles and Plantaris tendon	Tendon	*Mus musculus*	C57BL/6	No	8	8	457	6,643	3,271	273
E-PROT-75	PXD005230 [22]	Hippocampus, Cerebellum, Cortex	Brain	*Mus musculus*	C57BL/10J	Yes	72	36	7,663	63,479	41,683	6,037
E-PROT-76	PXD009909 [23]	Retina	Eye	*Mus musculus*	ND4 Swiss Webster	Yes	12	1	5,002	29,454	24,961	3,686
E-PROT-77	PXD012307 [24]	Lung	Lung	*Mus musculus*	C57BL/6	No	32	2	6,809	106,391	73,950	5,795
E-PROT-78	PXD009639 [25]	Lens	Eye	*Mus musculus*	CD1	Yes	10	1	4,519	20,779	18,006	3,064
E-PROT-79	PXD019394 [26]	Heart, Kidney, Liver, Lung, Brain, Spleen, Testis, Pancreas	Heart, Kidney, Liver, Lung, Brain, Spleen, Testis, Pancreas	*Mus musculus*	Swiss-Webster	Yes	96	8	9,853	141,506	105,701	8,185
E-PROT-81	PXD012636 [27]	Left atrium, Left ventricle, Right atrium, Right ventricle	Heart	*Mus musculus*	C57BL/6	Yes	120	4	7,772	146,966	99,577	6,435
E-PROT-82	PXD019431 [28]	Articular cartilage	Articular cartilage	*Mus musculus*	BALB\ c	No	72	6	1,815	17,695	15,191	1,518
E-PROT-83	PXD022614 [29]	Brain	Brain	*Mus musculus*	C57BL/6J: Rj C57BL/6JR ccHsd	Yes	120	6	6,645	97,443	69,884	5,673

E-PROT-84	PXD004496 [30]	Hippocampus	Brain	*Mus musculus*	C57BL/6J	Yes	204	17	4,192	37,363	30,100	3,424
E-PROT-85	PXD008736 [31]	Right atrium, Sinus node	Heart	*Mus musculus*	C57BL/6J	Yes	143	6	7,906	144,926	94,379	6,554
E-PROT-86§	PXD012677 [32]	Amygdala	Brain	*Rattus norvegicus*	Sprague Dawley	No	3	3	1,872	15,326	12,367	1,382
E-PROT-87§	PXD006692 [33]	Lung	Lung	*Rattus norvegicus*	Sprague Dawley	No	10	10	2,079	14,440	11,696	1,398
E-PROT-88§	PXD016793 [34]	Liver	Liver	*Rattus norvegicus*	Sprague Dawley	No	8	8	4,787	57,998	46,411	3,743
E-PROT-89§	PXD004364 [35]	Testis	Testis	*Rattus norvegicus*	Sprague Dawley	No	3	3	2,351	15,880	13,674	1,601
E-PROT-91	PXD001839 [36]	Left ventricle	Heart	*Rattus norvegicus*	F344/BN	No	12	12	1,345	10,310	8,804	925
E-PROT-92§	PXD013543 [37]	Left ventricle	Heart	*Rattus norvegicus*	Wistar	No	8	8	1,858	17,303	13,622	1,340
E-PROT-93	PXD016958 [38]	First segment of proximal tubule, second segment of proximal tubule, third segment of proximal tubule, medullary thick ascending limb, cortical thick ascending limb, distal convoluted tubule, connecting tubule, cortical collecting duct, outer medullary collecting duct, inner medullary collecting duct	Kidney	*Rattus norvegicus*	Sprague Dawley	Yes	132	32	7,846	103,886	83,662	6,130

E-PROT-94	PXD003375 [39]	Caudal and rostral segments of spinal cord	Spinal cord	*Rattus norvegicus*	Wistar	Yes	21	18	2,477	29,213	22,025	1,926
E-PROT-95§	PXD015928 [40]	Tendon	Tendon	*Rattus norvegicus*	Wistar	No	3	3	199	1,253	1,063	101
TOTAL	23 datasets (Mouse: 14, Rat: 9)	34 tissues (Mouse: 21, Rat: 18)	14 organs (Mouse: 12, Rat: 8)				1,173 MS runs (Mouse: 973, Rat: 200)	211 samples (Mouse: 114, Rat: 97)				

151

152

153 **Table 1.** List of mouse and rat proteomics datasets that were reanalysed. §Only normal/untreated samples within this dataset are reported in this

154 study. However, results from both normal and disease samples are available in Expression Atlas. † Numbers after post-processing.

155 **2.2. Protein coverage across organs and datasets**

156 One of our main aims was to study protein expression across various organs. To enable a
157 simpler comparison [14] we first grouped 34 different tissues into 14 distinct organs, as
158 discussed in 'Methods'. We defined 'tissue' as a distinct functional or structural region within
159 an 'organ'. We estimated the number of 'canonical proteins' identified across organs by first
160 mapping all members of each protein group to their respective parent genes. We defined the
161 parent gene as equivalent to the UniProt 'canonical protein' and we will denote the term
162 'protein abundance' to mean 'canonical protein abundance' from here on in the manuscript.

163

164 **2.2.1. Mouse proteome**

165 A total of 21,274 protein groups were identified from mouse datasets, among which 8,176
166 protein groups (38.4%) were uniquely present in only one organ and 70 protein groups
167 (0.3%) were ubiquitously observed (see the full list in Supplementary File 2). This does not
168 imply that these proteins are unique to these organs. Merely, this is the outcome considering
169 the selected datasets. Mouse protein groups were mapped to 12,570 genes (canonical
170 proteins) (Supplementary File 3). We detected the largest number of canonical proteins in
171 samples coming from liver (9,920, 78.9% of the total) and the lowest numbers in samples
172 from tendon (273, 2.2%) and articular cartilage (1,519, 12.1%) (Fig. 2A). In the case of
173 tendon and articular cartilage, both experiments did not include sample fractionation in their
174 sample preparation methodology, which can also explain the lower number of detected
175 proteins. The comparatively even lower number of proteins identified in tendon could be
176 attributed to the smallest sample size (only one sample out of 114, 0.9%). Also, tendon is a
177 relatively hypocellular tissue, which has a low protein turnover rate. Dataset PXD000867,
178 containing mouse liver samples, had the highest number of canonical proteins detected

179 (9,715, 77.3%), while the smallest number of proteins was detected in dataset PXD004612
180 (tendon, 273, 2.2%), as highlighted above (Fig. 2C).
181
182 We studied the normalised protein abundance distribution in organs (Fig. 2B) and found that
183 all organs, except tendon, had similar median abundances. However, one cannot attribute
184 further biological meaning to these observations, since by definition the method of
185 normalisation fixes each sample to have the same "total abundance", which then gets shared
186 out amongst all proteins. The normalised protein abundance distribution in datasets indicated
187 a higher than median abundances detected in datasets PXD004612 (tendon) and PXD003164
188 (testis) (Fig. 2D). A linear relationship was observed between the number of canonical
189 proteins detected in datasets and organs, when compared to the relative amount of their
190 spectral data (Fig. 2E). We found a significant number of proteins uniquely detected in one
191 organ (Fig. 2F). However, the list of concrete canonical proteins that were detected in just
192 one organ should be taken with caution since the list is subjected to inflated False Discovery
193 Rate (FDR), due to the accumulation of false positives when analysing the datasets
194 separately.
195 Some of the organs (liver, heart and brain) were represented across multiple mouse studies in
196 the aggregated dataset. A pairwise comparison of protein abundances in these organs
197 generally showed a good correlation in expression (heart: R^2 values ranged from 0.54 to 0.83;
198 brain: R^2 from 0.28 to 0.72; and liver: R^2 from 0.59 to 0.74) (Figure S1 in Supplementary File
199 4).
200
201

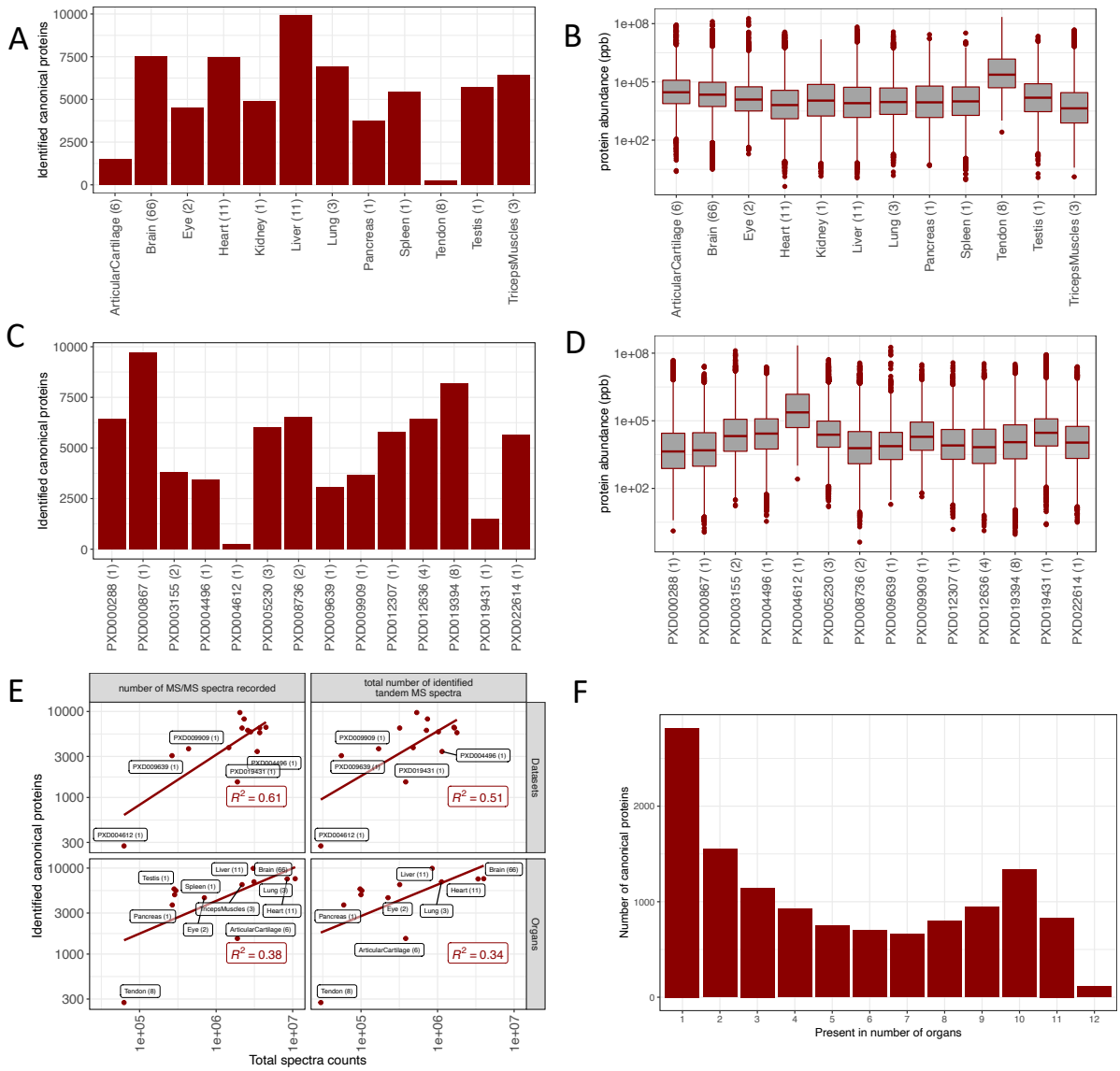

Figure 2. (A) Number of canonical proteins identified across different mouse organs. The number within the parenthesis indicates the number of samples. (B) Range of normalised iBAQ protein abundances across different organs. The number within the parenthesis indicates the number of samples. (C) Canonical proteins identified across different datasets. The number within the parenthesis indicate the number of unique tissues in the dataset. (D) Range of normalised iBAQ protein abundances across different datasets. The number within parenthesis indicate the number of unique tissues in the dataset. (E) Comparison of total spectral data with the number of canonical proteins identified in each dataset and organ. (F) Distribution of canonical proteins identified across organs.

212

213 **2.2.2. Rat proteome**

214 A total of 7,769 protein groups were identified across 8 different rat organs among which
215 3,649 (46.9%) protein groups were unique to one specific organ while 13 (0.16%) protein
216 groups were present among all organs (see full list in Supplementary File 2). The protein
217 groups were mapped to 7,116 genes (canonical proteins) (Supplementary File 3). The highest
218 number of canonical proteins (6,106, 85.1%) was found in rat kidney samples. The lowest
219 number of canonical proteins (101, 1.4%) was found in samples from tendon, as shown in
220 Fig. 3A. The largest number of canonical proteins identified in kidney is likely because of the
221 relatively large number of samples (32 samples), when compared to other organs. However, it
222 is interesting to note that large numbers of canonical proteins were detected in liver samples,
223 which relatively had fewer number of samples, when compared to the total number of
224 samples in heart and spinal cord.

225

226 Datasets PXD016958 and PXD016793 consisted entirely of kidney (where fractionation was
227 performed) and liver (no fractionation) samples, respectively, and as mentioned above had
228 the largest number of canonical proteins identified (Fig. 3C). The normalised protein
229 abundances were similar among the various organs and datasets (Fig. 3B, D). We also
230 observed a linear relation between the number of canonical proteins identified and the MS
231 spectra identified (Fig. 3E). As seen in the mouse datasets, we also observed a large number
232 of proteins uniquely detected in one organ (Fig. 3F). As highlighted above, the list of
233 concrete canonical proteins that were detected in just one organ should be taken with caution
234 since the list is subjected to inflated False Discovery Rate (FDR).

235 In the case of rat datasets, left ventricle heart samples were the only ones represented in more
236 than one study (PXD001839 and PXD013543) in the aggregated dataset. A pairwise

237 comparison of protein abundances of heart between these two datasets was performed,

238 showing a strong correlation in protein expression ($R^2 = 0.9$) (Figure S1D in Supplementary

239 File 4).

240

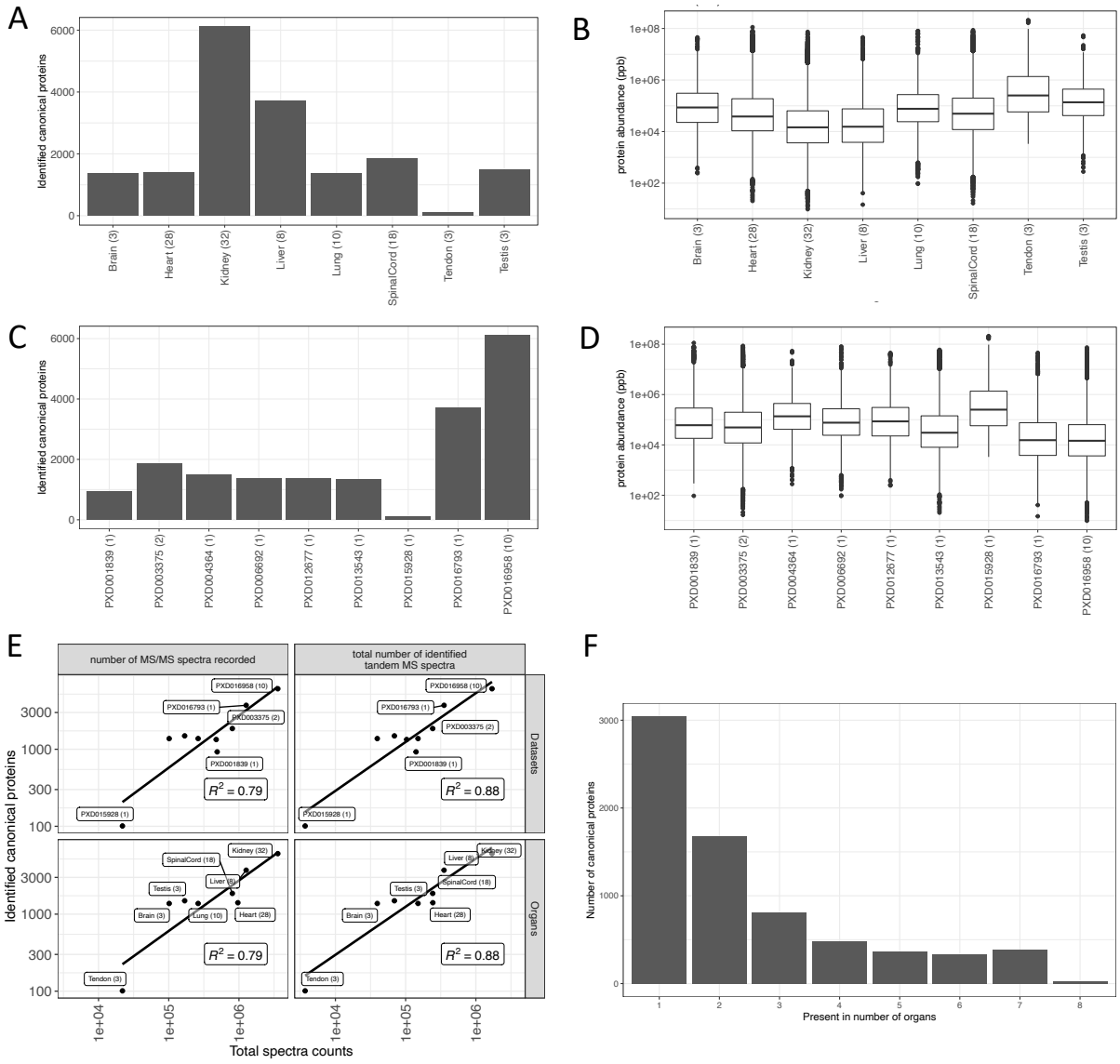

241

242 **Figure 3.** (A) Number of canonical proteins identified across different rat organs. The

243 number within the parenthesis indicates the number of samples. (B) Range of normalised

244 iBAQ protein abundances across different organs. The number within the parenthesis

245 indicates the number of samples. (C) Canonical proteins identified across different datasets.

246 The number within the parenthesis indicate the number of unique tissues in the dataset. (D)

247 Range of normalised iBAQ protein abundances across different datasets. The number within
248 parenthesis indicate the number of unique tissues in the dataset. (E) Comparison of total
249 spectral data with the number of canonical proteins identified in each dataset and organ. (F)
250 Distribution of canonical proteins identified across organs.
251
252 **2.3. Protein abundance comparison across organs**
253 Next, we studied how protein abundances compared across different datasets and organs. The
254 presence of batch effects between datasets makes this type of comparisons challenging. To
255 aid comparison of protein abundances between datasets we transformed the normalised iBAQ
256 intensities into ranked bins as explained in 'Methods', i.e., proteins included in bin 5 are
257 highly abundant whereas proteins in bin 1 are expressed in the lowest abundances (among the
258 detected proteins).
259
260 **2.3.1. Mouse proteome**
261 We found that 1,086 (8.6%) proteins were found with their highest level of expression in at
262 least 3 organs, with a median bin value greater than 4 (Supplementary File 3). On the other
263 end of the scale, 138 (1.1%) canonical proteins were found with their lowest expression in at
264 least 3 organs, with a median bin value of less than 2. The bin transformed abundances in all
265 organs are provided in Supplementary File 3.
266
267 To compare protein expression across all organs, we calculated pairwise Pearson correlation
268 coefficients across 117 samples (Fig. 4A). We observed some correlation in protein
269 expression within brain (median $R^2 = 0.31$) and a higher one in heart (median $R^2 = 0.67$)
270 samples. We performed Principal Component Analysis (PCA) on all samples from mouse
271 datasets for testing the effectiveness of the bin transformation method in reducing batch

effects. Fig. 4B shows the clustering of samples from various organs of mouse. We observed samples from the same organ generally clustered together. For example, we observed that brain samples all clustered together in one group, even though they come from different datasets, indicating decent removal of batch effects (Fig. 4C). However, we also observed that samples from other organs such as liver did not cluster according to their organ types but clustered together within the dataset they were part of, indicating some residual batch effects, which are hard to remove completely.

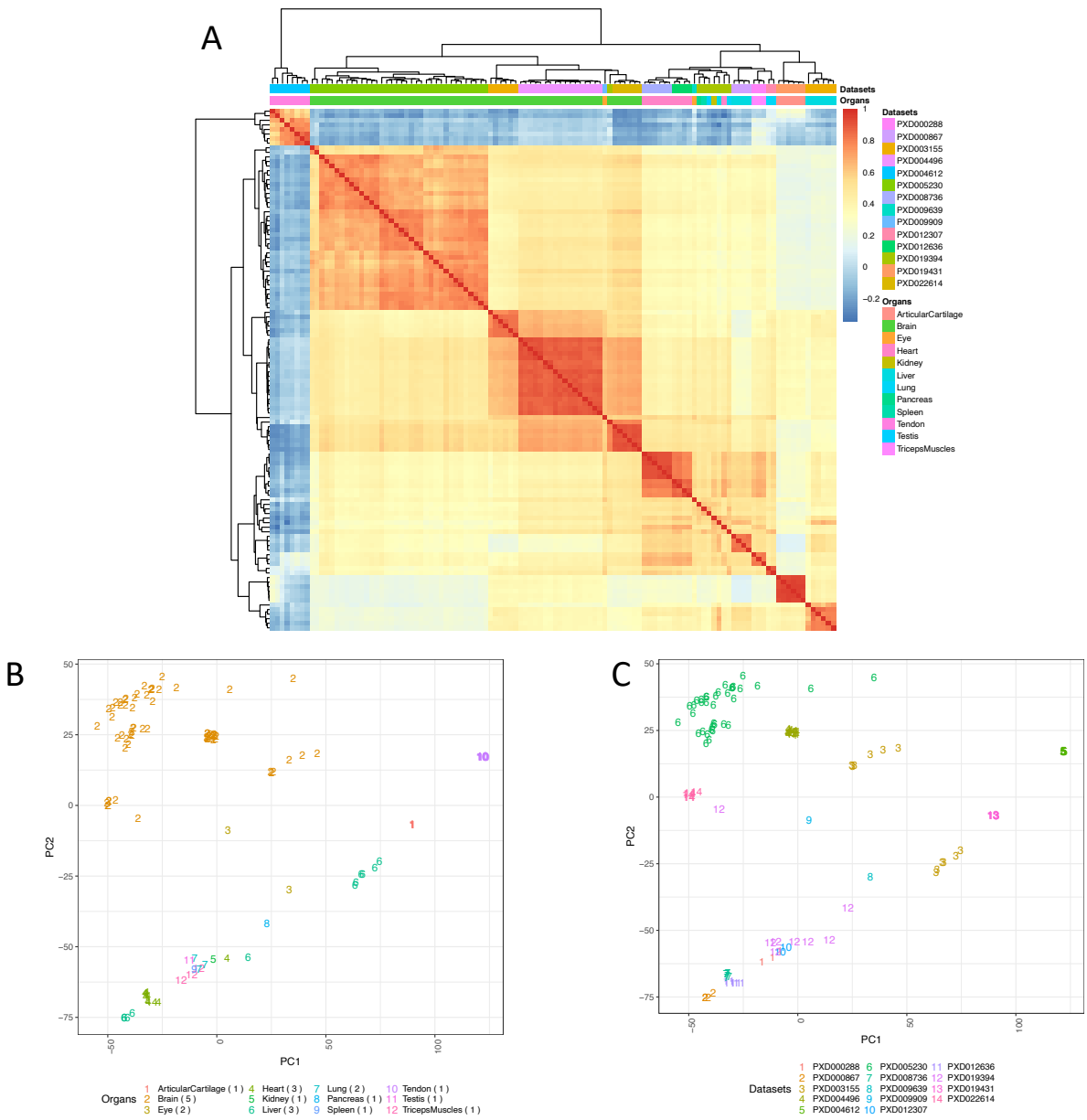

281 **Figure 4.** (A) Heatmap of pairwise Pearson correlation coefficients across all mouse samples.
282 The colour represents the correlation coefficient and was calculated using the bin transformed
283 iBAQ values. The samples were hierarchically clustered on columns and rows using
284 Euclidean distances. (B) PCA of all samples, using the binned protein abundances as input,
285 coloured by the organ types. (C) PCA of all samples coloured by their respective dataset
286 identifiers. The numbers in parenthesis indicate the number of datasets for each organ.
287 Binned values of canonical proteins quantified in at least 50% of the samples were used to
288 perform the PCA.
289
290 In addition, we compared the protein abundances generated in this study with the data
291 available in the resource PaxDB generated using spectral counting across different mouse
292 organs. We observed generally a strong correlation of protein abundances calculated using
293 iBAQ from this study (fraction of total (FOT) normalised ppb) and spectral counting methods
294 (Figure S2 in Supplementary File 4). However, the expression of low abundant proteins
295 seemed to be underestimated in PaxDB when compared with our results, as shown by a S-
296 shaped curve in the scatterplot in organs such as brain, heart, liver and lung. The 'dynamic
297 exclusion' [41] setting used by modern mass spectrometers prevents the instrument from
298 fragmenting abundant peptides multiple times when they are repeatedly observed in scans
299 nearby in time. This has the effect that spectral counting approaches will limit the dynamic
300 range observed, as high abundant proteins will be under sampled. This is a limitation when
301 using spectral counting methods, and these days spectral counting is not commonly used as a
302 truly quantitative data type in proteomics.
303
304 **2.3.2. Rat proteome**

305 Next, we studied the distribution of protein abundances across organs in rat. On one hand,
306 311 (4.3%) proteins were found with their highest expression in at least 3 organs with a
307 median bin value greater than 4. On the other hand, 27 (0.37%) canonical proteins were
308 found with their lowest expression in at least 3 organs, with a median bin value of less than 2.
309 The bin transformed abundances in all organs are provided in Supplementary File 3.
310 Overall, the samples from rat datasets showed a better correlation in protein expression (Fig.
311 5A) than in the case of mouse. We observed generally a strong correlation of protein
312 expression within samples from liver (median Pearson's correlation $R^2 = 0.85$), lung (median
313 $R^2 = 0.71$), spinal cord (median $R^2 = 0.65$), heart (median $R^2 = 0.71$) and brain (median $R^2 =$
314 0.86). We also observed the clustering in the PCA of samples coming from the same organ
315 (Fig. 5B). Kidney, lung, spinal cord and heart samples all clustered together according to
316 their organ type. Fig. 5C shows the samples based on the dataset they were part of. However,
317 most organ samples were part of individual datasets except in the case of samples from heart,
318 which came from two datasets (PXD001839 and PXD013543). Fig. 5C shows that the heart
319 samples clustered into two nearby groups (bottom left two clusters on Fig. 5B and 5C),
320 wherein each cluster included samples from a different dataset, indicating the presence of
321 small batch effects.

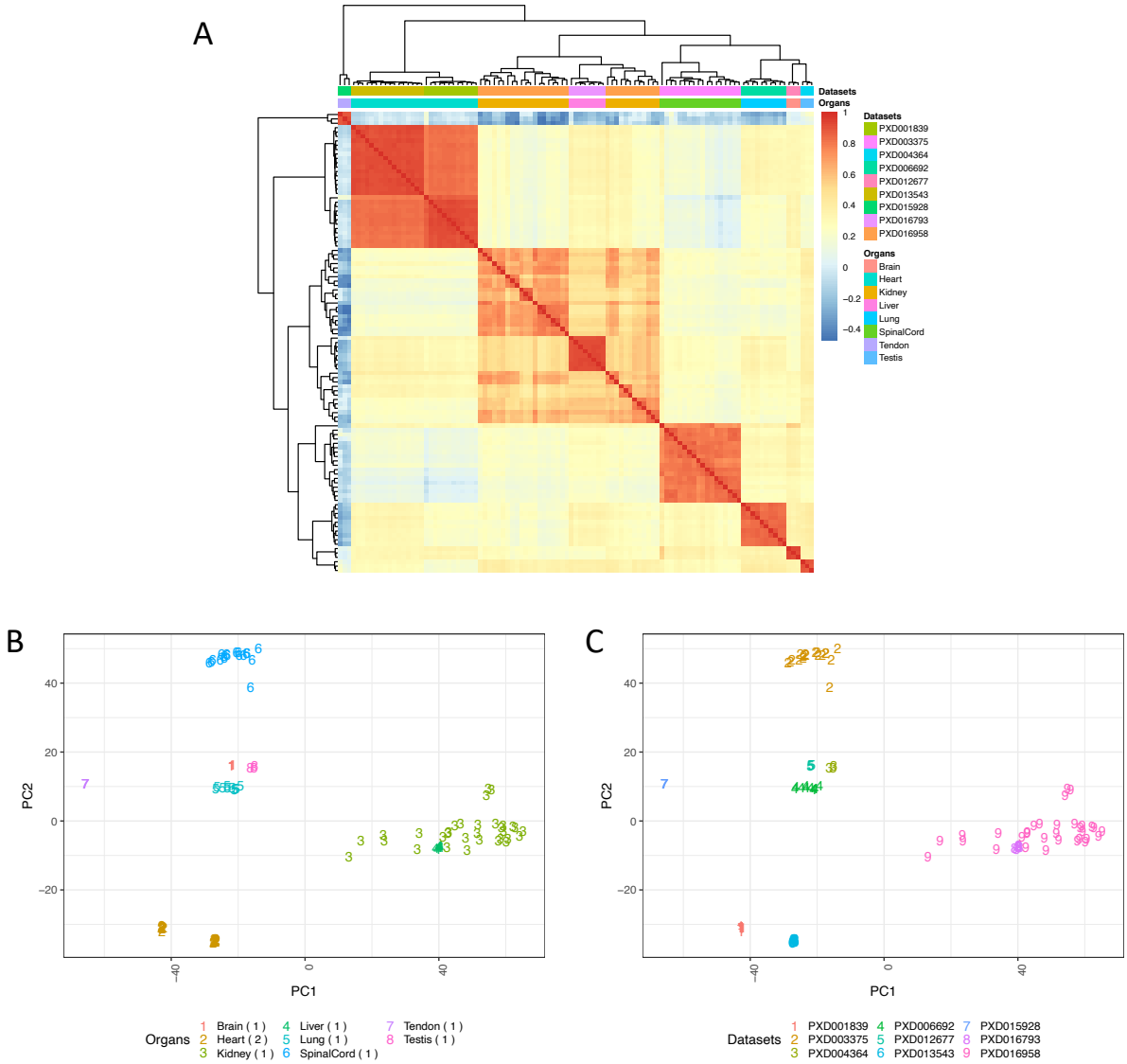

Figure 5. (A) Heatmap of pairwise Pearson correlation coefficients across all rat samples. The colour represents the correlation coefficient and was calculated using the bin transformed iBAQ values. The samples were hierarchically clustered on columns and rows using Euclidean distances. (B) PCA of all samples coloured by the organ types. (C) PCA of all samples coloured by their respective dataset identifiers. The numbers in parenthesis indicate the number of datasets for each organ. Binned values of canonical proteins quantified in at least 50% of the samples were used to perform the PCA.

2.4. The organ elevated proteome and the over-representative biological processes

332 Based on their expression, canonical proteins were classified into three different groups based
333 on their organ specificity: “mixed”, “group-enriched” and “organ-enriched” (see
334 Supplementary File 5). We considered over-expressed canonical proteins in each organ as
335 those which were in “group-enriched” and “organ-enriched”. The analysis showed that on
336 average, 20.8% and 26.0% of the total elevated canonical proteins were organ group-specific
337 in mouse and rat, respectively (Fig. 6). In addition, 4.3% and 14.2% were unique organ-
338 enriched in mouse and rat, respectively. The highest ratio of organ-enriched in mouse was
339 found in liver (13.6%), whereas in rat, it was found in kidney (39.8%).

340 We then performed a gene ontology (GO) enrichment analysis of those proteins that were
341 'organ-enriched' and group-enriched' using GO terms associated with biological processes.
342 We found 1,036 GO terms to be statistically significant in all organs, as seen in
343 Supplementary File 6. The most significant GO terms for each organ are shown in Table 2.
344

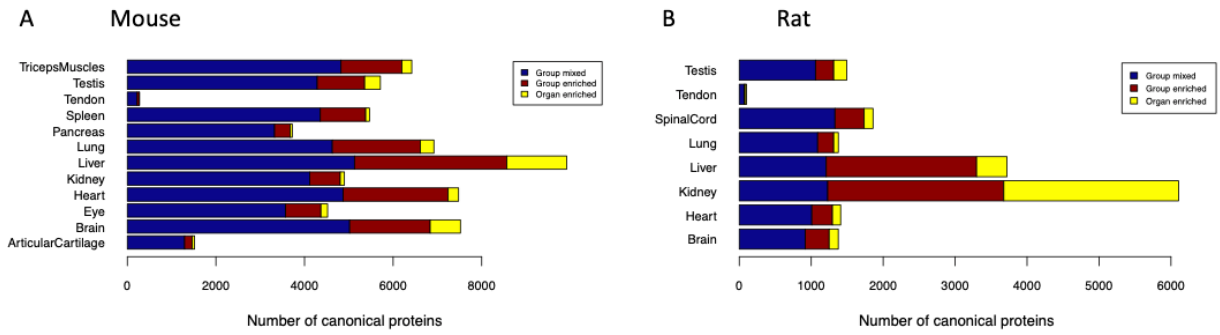

345

346 **Figure 6.** Organ specificity of canonical proteins in (A) mouse and (B) rat.

347

Organ	Species	GO ID	Description	adjusted p-value
Articular cartilage	*Mus musculus*	GO:0030198 GO:0043062 GO:0045229	Extracellular matrix organization Extracellular structure organization External encapsulating structure organization	$8.94*10^{-38}$ $8.94*10^{-38}$ $8.94*10^{-38}$
Brain	*Mus musculus*	GO:0050804 GO:0099177 GO:0050808	Modulation of chemical synaptic transmission Regulation of trans-synaptic signalling Synapse organization	$7.03*10^{-65}$ $7.03*10^{-65}$ $1.41*10^{-48}$

Heart	*Mus musculus*	GO:0060047 GO:0008016 GO:0060537	Heart contraction Regulation of heart contraction Muscle tissue development	$7.10*10^{-11}$ $4.43*10^{-10}$ $6.16*10^{-10}$
Kidney	*Mus musculus*	GO:0015711 GO:0044282 GO:0016054	Organic anion transport Small molecule catabolic process Organic acid catabolic process	$4.59*10^{-19}$ $4.91*10^{-15}$ $6.25*10^{-15}$
Eye	*Mus musculus*	GO:0007601 GO:0001654 GO:0099504	Visual perception Eye development Synaptic vesicle cycle	$7.54*10^{-50}$ $5.31*10^{-31}$ $8.36*10^{-18}$
Liver	*Mus musculus*	GO:0016569 GO:0016570 GO:0019369	Covalent chromatin modification Histone modification Arachidonic acid metabolic process	$6.26*10^{-10}$ $1.71*10^{-08}$ $1.71*10^{-08}$
Lung	*Mus musculus*	GO:0120031 GO:0030031 GO:0044782	Plasma membrane bounded cell projection assembly Cell projection assembly Cilium organization	$3.61*10^{-14}$ $3.61*10^{-14}$ $9.83*10^{-14}$
Pancreas	*Mus musculus*	GO:0007586 GO:0032328	Digestion Alanine transport	0.005 0.018
Spleen	*Mus musculus*	GO:0046649 GO:0050776 GO:0045087	Lymphocyte activation Regulation of immune response Innate immune response	$4.12*10^{-22}$ $2.00*10^{-20}$ $2.23*10^{-20}$
Tendon	*Mus musculus*	GO:0003012 GO:0050879 GO:0050881	Muscle system process Multicellular organismal movement Musculoskeletal movement	$1.46*10^{-25}$ $3.14*10^{-19}$ $1.46*10^{-25}$
Testis	*Mus musculus*	GO:0048232 GO:0003341 GO:0044782	Male gamete generation Cilium movement Cilium organization	$8.75*10^{-49}$ $3.04*10^{-38}$ $6.78*10^{-37}$
Triceps muscles	*Mus musculus*	GO:0061061 GO:0055002 GO:0003009	Muscle structure development Striated muscle cell development Skeletal muscle contraction	$1.56*10^{-14}$ $2.41*10^{-14}$ $3.53*10^{-14}$
Brain	*Rattus norvegicus*	GO:0099537 GO:0007268 GO:0098916	Trans-synaptic signalling Chemical synaptic transmission Anterograde trans-synaptic signalling	$1.79*10^{-60}$ $1.79*10^{-60}$ $1.79*10^{-60}$
Heart	*Rattus norvegicus*	GO:0061061 GO:0003012 GO:0055001	Muscle structure development Muscle system process Muscle cell development	$2.94*10^{-17}$ $6.30*10^{-16}$ $4.00*10^{-15}$
Kidney	*Rattus norvegicus*	GO:0006396 GO:0045944 GO:0006260	RNA processing positive regulation of transcription by RNA polymerase II DNA replication	$6.19*10^{-13}$ $7.29*10^{-06}$ $1.74*10^{-05}$
Liver	*Rattus norvegicus*	GO:0008202 GO:0016054 GO:0032787	Steroid metabolic process Organic acid catabolic process Monocarboxylic acid metabolic process	$2.74*10^{-10}$ $1.61*10^{-09}$ $1.64*10^{-09}$
Lung	*Rattus norvegicus*	GO:0031589 GO:0009617 GO:0030036	Cell-substrate adhesion Response to bacterium Actin cytoskeleton organization	$7.62*10^{-08}$ $7.62*10^{-08}$ $1.40*10^{-07}$
Spinal cord	*Rattus norvegicus*	GO:0061564 GO:0099537 GO:0007268	Axon development Trans-synaptic signalling Chemical synaptic transmission	$4.26*10^{-18}$ $5.93*10^{-16}$ $5.93*10^{-16}$
Tendon	*Rattus norvegicus*	GO:0030199 GO:0061448 GO:0001501	Collagen fibril organization Connective tissue development Skeletal system development	$1.23*10^{-13}$ $2.31*10^{-09}$ $3.39*10^{-09}$

Testis	*Rattus norvegicus*	GO:0019953 GO:0051704 GO:0007018	Sexual reproduction Multi-organism process Microtubule-based movement	$3.98*10^{-24}$ $1.61*10^{-18}$ $4.00*10^{-12}$

348

349 **Table 2.** Analysis of the top three GO terms for each organ in mouse and rat using the
350 elevated organ-specific and group-specific canonical proteins as described in the 'Methods'
351 section.

352

353 **2.5. Protein abundances across orthologs in three species**

354 In a previous study, we analysed 25 label-free proteomics datasets from healthy human
355 samples to assess baseline protein abundances in 14 organs following the same analytical
356 methodology [14]. We compared the expression of canonical proteins identified in all three
357 species (rat, mouse and human). Overall, 13,248 detected human genes (corresponding to the
358 canonical proteins) were compared with 12,570 genes detected in mouse and 7,116 genes
359 detected in rat. The number of orthologous mappings (i.e., "one-to-one" mappings, see
360 'Methods') between rat, mouse and human genes are listed in table 3. We only considered
361 one-to-one mapped orthologues for the comparison of protein abundances.

362

Species	**Identified genes**	**Orthologs of human genes identified in [14]**	**Percentage of genes with different mapping against identified human genes**				
			one-to-one	**one-to-many**	**many-to-many**	**many-to-one**	**not mapped**
Mus musculus	12,570	10,601	80.4%	1.9%	0.56%	1.46%	15.7%
Rattus norvegicus	7,116	6,058	82.0%	2.2%	0.70%	0.25%	14.9%

363

364 **Table 3.** Homologs identified in mouse and rat datasets when compared with the background
365 list of genes (corresponding to canonical proteins) identified in human datasets
366 (Supplementary File 2 in [14]).

367

368 Among human and mouse orthologues we observed relatively high levels of correlation of
369 protein abundances in brain (R^2 = 0.61), heart (R^2 = 0.65) and liver (R^2 = 0.56) (Fig. 7A).
370 Human and rat orthologs showed also relatively high levels of correlation in brain (R^2 =
371 0.62), kidney (R^2 = 0.53) and liver (R^2 = 0.56), but almost no correlation in lung (R^2 = 0.12)
372 and testis (R^2 = 0.18) (Fig. 7B). Between mouse and rat orthologs, the correlation of protein
373 abundances was higher in liver (R^2 = 0.65), kidney (R^2 = 0.54) and brain (R^2 = 0.57) samples,
374 when compared to the samples coming from the rest of the organs (Fig. 7C). Fig. 7D shows
375 an illustration of some example comparisons of individual orthologs using binned protein
376 abundances.

377

378 For the same corresponding subsets, we also investigated the correlation of protein
379 expression between various organs within each organism. We observed that in general the
380 correlation of protein expression was slightly lower between organs within the same species,
381 when compared to a higher correlation, which was observed among orthologs (Figure S3 in
382 Supplementary File 4). The found lower correlation of protein expression between different
383 organs was more apparent in mouse and rat.

384

385 Among the orthologs expressed in all organs in all three species, 747 (12.3%) orthologs were
386 detected with a median bin expression value of more than 4, i.e., proteins that appear to have
387 conserved high expression in all organs and all tissues. Additionally, 13 (0.2%) orthologs
388 were found with a median bin expression value less than 2 in all organs, although, it is harder
389 to detect consistently proteins with low abundances across all organs. A full list of the binned
390 protein abundances of orthologs is available in Supplementary File 7. The illustration of all
391 binned protein abundances across the three species is shown in Supplementary File 8.

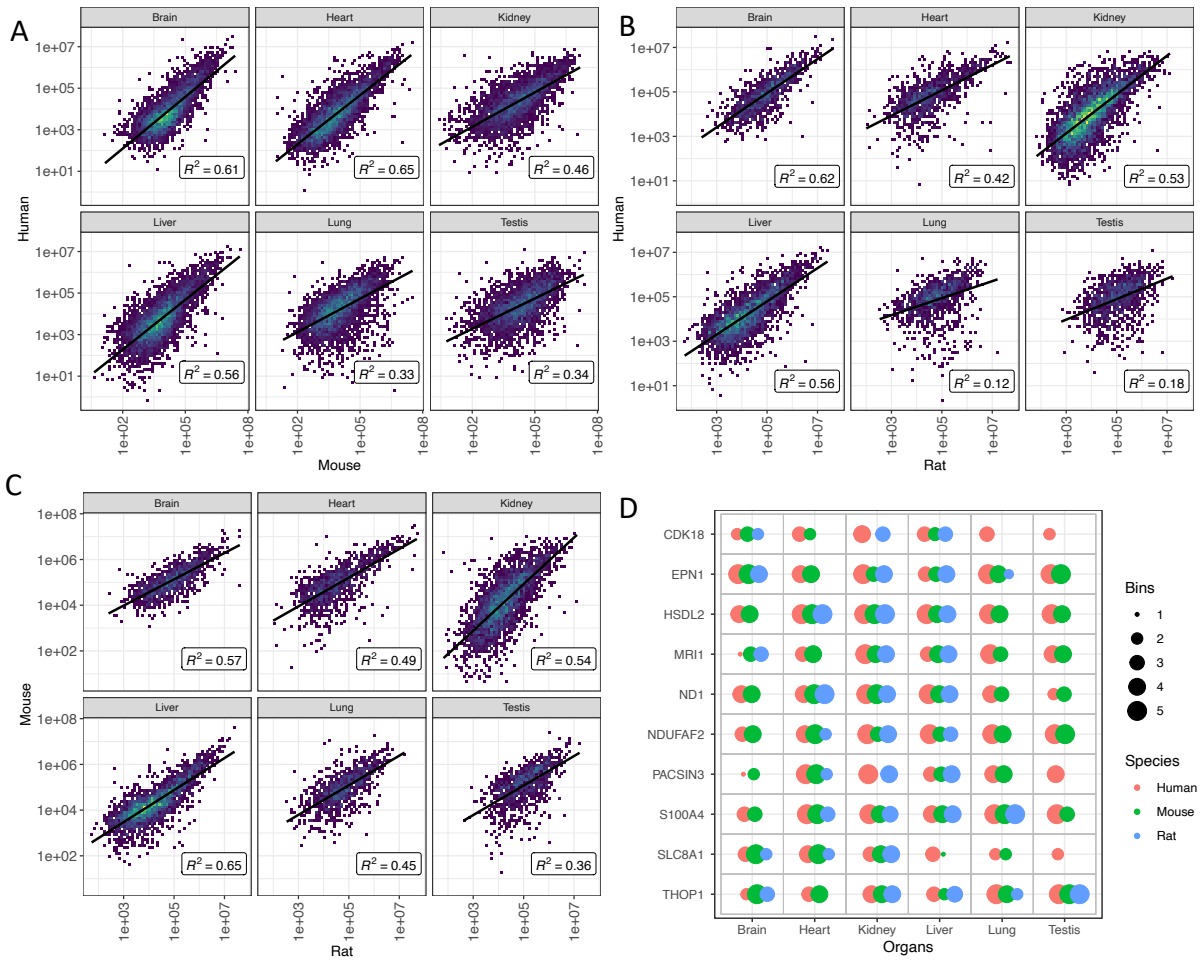

Figure 7. Comparison of protein abundances (in ppb) between one-to-one mapped orthologs of mouse, rat and human in various organs. (A) Pairwise correlation using normalised protein abundances of human and mouse orthologues. (B) Human and rat orthologs. (C) Mouse and rat orthologs. (D) As an example, the comparisons of binned protein expression of ten randomly sampled orthologs are shown. Data corresponding to all cases (as reported in panel D) are available in Supplementary File 7 and the corresponding illustration of binned values is available in Supplementary File 8. Orthologs in (D) are shown using their human gene symbol.

Since each sample contains potentially thousands of protein values this creates a high level of dimensionality within the data. To reduce this, we used the non-linear dimension reduction

404 algorithm, Uniform Manifold Approximation and Projection (UMAP) (see Section 4.7 in the
405 'Methods' section). The UMAP algorithm enables the reduction of multidimensional data to
406 a two-dimensional space upon which the relationship between each sample can be visualised.
407 Specifically, it enables the visualisation of the relationships of proteins across individual
408 samples and organs. Should multiple samples be positioned near to each other, it allows for
409 us to predict that these samples shared similar properties (in this case, similar protein
410 abundance values). Consequently, by overlaying samples from various species UMAP
411 representations can be used to visualise the relationship of various orthologs across similar
412 organs.

413 Using the UMAP algorithm, we were able to visualise the relationships between individual
414 organs regardless of the involved species (human, mouse, rat) and to identify similar genes
415 (corresponding to canonical proteins) within those organs. The overall view of all samples
416 labelled by their respective organ is shown as Figure 8A. We chose to use the biological
417 system as the basis for the colouring scheme for each sample to reduce the overall complexity
418 of the visualisation, due the high number of organs included. By using this labelling scheme,
419 we could see that the clustering of each sample was deterministic. Each sample was
420 positioned within a clear region for the corresponding organs, despite the original layout
421 being unaware of this information. This indicates that not only do the samples within those
422 organs share common protein abundance values, but furthermore, that samples that come
423 from the same organs share similar protein expression (as three species are present).

424 Furthermore, in Figure 8B we show the representation of binned protein abundance values for
425 three example genes (SH3GL2, MYOZ2 and PYROXD2), providing information on the
426 abundance of them across different biological systems. These visualisations use the same
427 layout than within Figure 8A. In the example of SH3GL2, it can be seen that Figure 8B

428 shows multiple values that have been scored as bin 5. By referring to Figure 8A, we can see
429 that those points corresponding to highly abundant proteins, come from samples from the
430 nervous system (in all three species). Furthermore, using the same method, it can be seen that
431 MYOZ2 is highly abundant in the circulatory system, and that PYROXD2 is highly abundant
432 in the urinary system. The UMAP coordinates and our binned protein abundance data that is
433 used in these plots to allow for the generation of similar visualisations are provided in
434 Supplementary File 9.

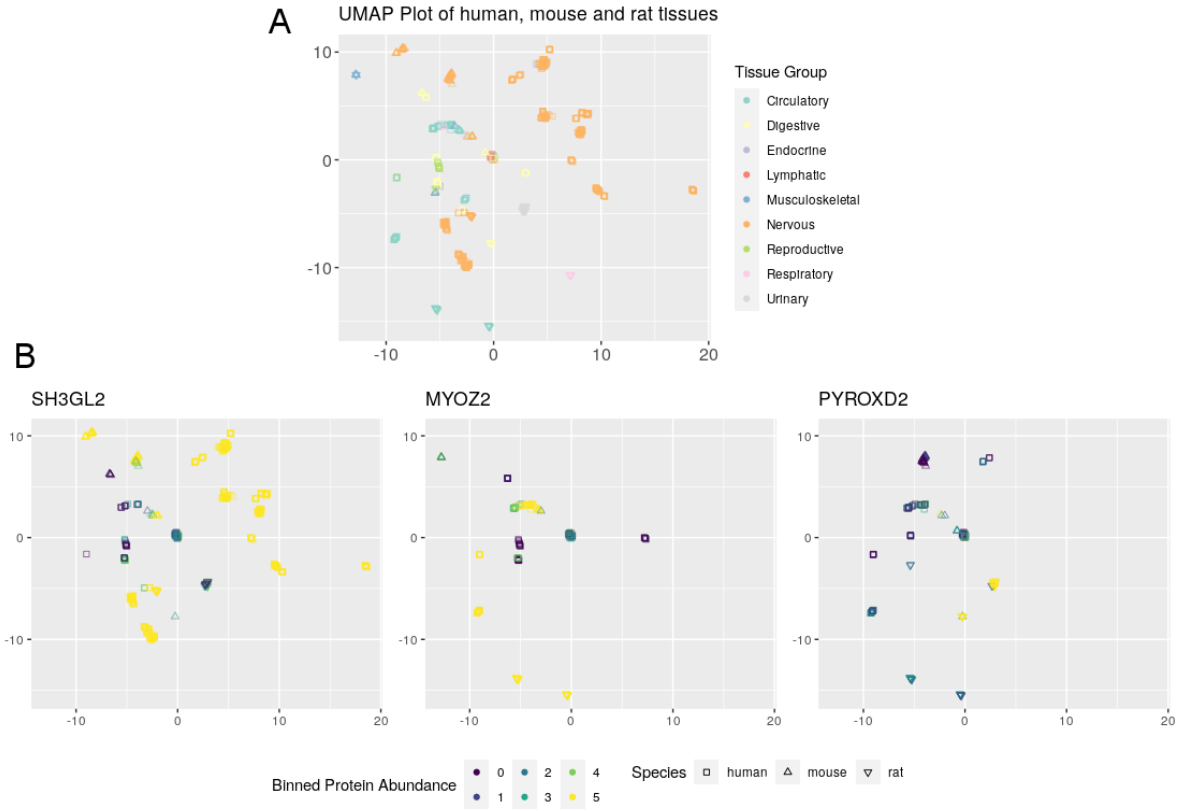

435

436 **Figure 8:** Visualisations generated using the UMAP algorithm to show the relationships
437 between human, mouse, and rat samples. (**A**) Shows the relationship of all samples,
438 particularly showing strong relationship between biological systems. **(B)** Shows the protein
439 abundancy of 3 example gene orthologs (SH3GL2, MYOZ2 and PYROXD2), within each
440 sample. Human baseline protein expression data was generated in [14].
441

442 **2.6. Pathway enrichment analysis**

443 Based on the ortholog protein expression analysis described above, we mapped canonical
444 proteins from mouse and rat to the corresponding ortholog human proteins, which were
445 subsequently subjected to pathway-enrichment analysis using Reactome (Fig. 9). After
446 filtering out the disease and statistically insignificant pathways, there were 2,990 pathways
447 found in all the organs of mouse and 2,162 pathways in all the organs of rat. In mouse
448 samples, the largest number of pathways (367) were found in articular cartilage, and the
449 lowest number of pathways was found in liver (44). We also observed that Neuronal System-
450 related pathways were predominantly present in the brain and eye, which is consistent with
451 expectations. In rat samples, brain included the largest number of pathways (387), while the
452 lowest number of pathways was found in tendon, with 117.

453

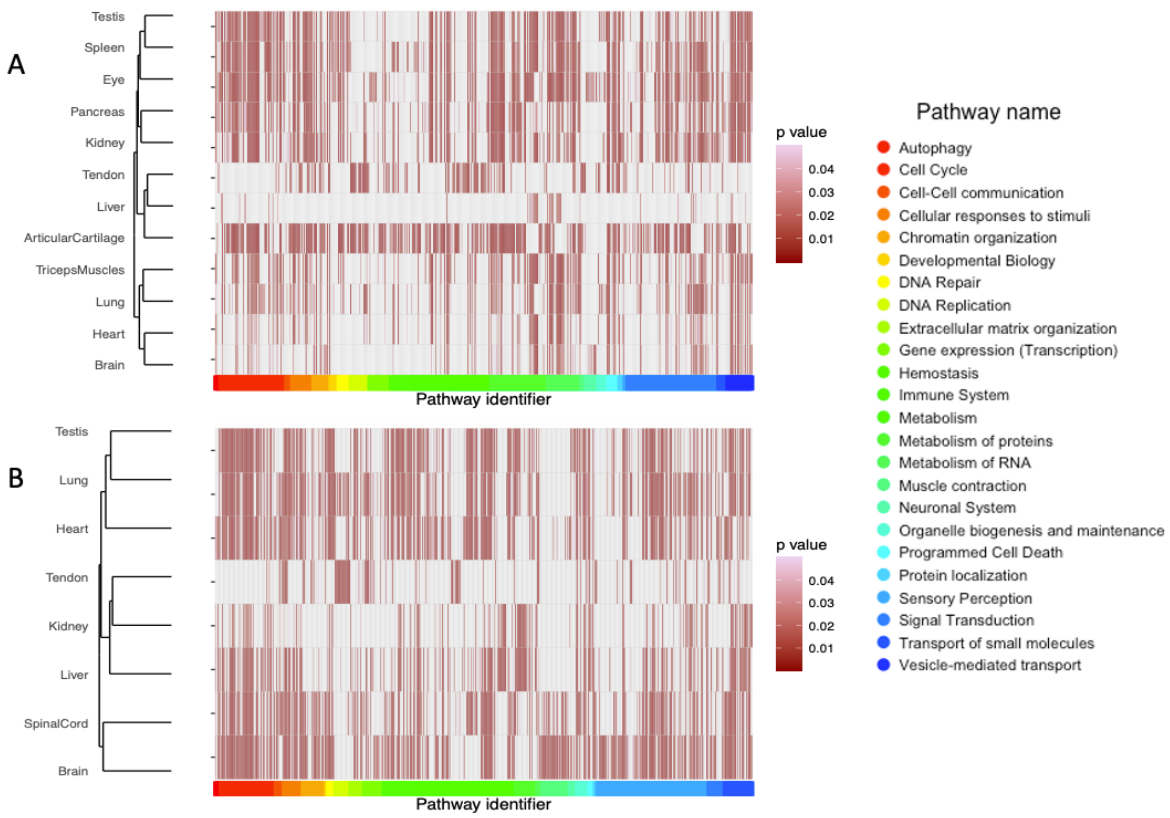

454

455 **Figure 9.** Pathway analysis performed using the canonical proteins, showing the statistically

456 significant representative pathways (p-value < 0.05) in (A) mouse and (B) rat organs.

457 **3. Discussion**

458 We have previously reported two meta-analysis studies involving the reanalysis and
459 integration in Expression Atlas of public quantitative datasets coming from cell lines and
460 human tumour samples [13], and from human baseline tissues [14], respectively. In this
461 study, we reanalysed mouse and rat baseline proteomics datasets representing protein
462 expression across 34 healthy tissues and 14 organs. We have used the same methodology as
463 in the study involving baseline human tissues, which enabled a comparison of protein
464 expression levels across the three species. Our main overall aim was to provide a system-
465 wide baseline protein expression catalogue across various tissues and organs of mouse and rat
466 and to offer a reference for future related studies.

467

468 We analysed each dataset separately using the same software (MaxQuant) and the same
469 search protein sequence database. The disadvantage of this approach is that the FDR
470 statistical thresholds are applied at a dataset level and not to all datasets together as a whole.
471 However, as reported before [14], using a dataset per dataset analysis approach is in our view
472 the only sustainable manner to reanalyse and integrate quantitative proteomics datasets, at
473 least at present. The disadvantage of this approach is that the FDR statistical threshold are
474 applied at a dataset level and not to all datasets together as a whole, with the potential
475 accumulation of false positives across datasets. However, it is important to highlight that the
476 number of commonly detected false positives is reduced in parallel with the increase in the
477 number of common datasets where a given protein is detected. As also reported in previous
478 studies, one of the major bottlenecks was the curation of dataset metadata, consisting of
479 mapping files to samples and biological conditions. Very recently, the MAGE-TAB-
480 Proteomics format has been developed and formalised to enable the reporting of the
481 experimental design in proteomics experience, including the relationship between samples

482 and raw files, which is recorded in the SDRF-Proteomics section of the file [42]. Submission
483 of the SDRF-Proteomics files to PRIDE is now supported. The more well-annotated datasets
484 in the public domain, the easier these data reuse activities will become.
485
486 The generated baseline protein expression data can be used with different purposes such as
487 the generation of protein co-expression networks and/or the inference of protein complexes.
488 For the latter application, expression data can be alone or for potentially refining predictions
489 obtained using different methods such as the recently developed AlphaFold-based protein
490 complexes predictions [43]. Mouse and rat are widely used species in the context of drug
491 discovery, the latter especially, to undertake regulatory pre-clinical safety studies. Therefore,
492 it is important to know quantitative protein expression distribution in these species in
493 different tissues [44] to assist in the selection of species for such studies and also for the
494 interpretation of the final results.
495
496 In addition to the analyses reported, it would have also been possible to perform correlation
497 studies between gene and protein expression information. However, we did not find any
498 relevant public datasets in the context of this manuscript where the same samples were
499 analysed by both techniques, which is the optimal way to perform these studies. Future
500 directions in analogous studies will involve: (i) additional baseline protein expression studies
501 of other species, including other model organisms or other species of economic importance;
502 (ii) the inclusion of differential proteomics datasets (e.g. using TMT and/or iTRAQ); and (iii)
503 include relevant proteomics expression data coming from the reanalysis of Data Independent
504 Acquisition (DIA) datasets [45].
505

506 As mentioned above, we performed a comparative analysis of baseline protein expression
507 across human, mouse and rat. It was possible to perform this analysis for six common organs
508 (brain, heart, kidney, liver, lung and testis). Ortholog expression across species is useful to
509 infer protein function across experimentally studied proteins. This is particularly useful as
510 evolutionarily closely related species are likely to conserve protein function. We could not
511 find in the literature an analogous comparative study performed at the protein level.
512 However, expression from closely related orthologs across tissues or organs has been
513 compared at the transcriptomics level, providing a complete picture of gene expression. In
514 this context, many studies have compared gene-expression in mouse, rat and human
515 orthologues and found that orthologues had generally a highly correlated expression tissue
516 distribution profile in baseline conditions [46-50]. Gene expression levels among orthologs
517 were found to be highly similar in muscle and heart tissues, liver and nervous system and less
518 similar in epithelial cells, reproductive systems, bone and endocrine organs [48]. Studies have
519 also shown that variability of gene expression between homologous tissues/organs in closely
520 related species can be lower than the variability between unrelated tissues within the same
521 organism [46, 47], in agreement with the results reported here at the protein level.
522 Additionally, we showed an initial analysis of protein expression of orthologs across the three
523 species using UMAP.
524
525 In conclusion we here present a meta-analysis study of public mouse and rat baseline
526 proteomics datasets from PRIDE. We demonstrate its feasibility, perform a comparative
527 analysis across the three species and show the main current challenges. Finally, the data is
528 made available *via* Expression Atlas. Whereas there are several analogous studies performed
529 at the gene expression level for mouse and rat tissues, to the best of our knowledge this is the
530 first of this kind at protein expression level.

531 **4. Materials and Methods**

532

533 **4.1. Datasets**

534 As of May 2021, there were 2,060 mouse (*Mus musculus*) and 339 rat (*Rattus norvegicus*)
535 MS proteomics datasets publicly available in the PRIDE database
536 (https://www.ebi.ac.uk/pride/). Datasets were manually selected based on the selection
537 criteria described previously [14]. Briefly, we selected datasets where baseline expression
538 experiments were performed on (i) label-free samples from tissues not enriched for post-
539 translational modifications; (ii) Thermo Fisher Scientific instruments such as LTQ Orbitrap,
540 LTQ Orbitrap Elite, LTQ Orbitrap Velos, LTQ Orbitrap XL ETD, LTQ-Orbitrap XL ETD,
541 Orbitrap Fusion and Q-Exactive, since they represent a large proportion of datasets in PRIDE
542 and to avoid heterogeneity introduced by data from other vendor instruments; (iii) had
543 suitable sample metadata available in the original publication or it was possible to obtain it by
544 contacting the authors; and (iv) our previous experience in the team of some datasets
545 deposited in PRIDE, which were discarded because they were not considered to be useful.
546 Overall, 14 mouse and 9 rat datasets were selected from all mouse and rat datasets for further
547 analysis. Table 1 lists the selected datasets. The 23 datasets contained a total of 211 samples
548 from 34 different tissues across 14 organs (meaning groups of related tissues, more details
549 below), comprising 9 different mouse and 3 rat strains, respectively.
550 The sample and experimental metadata were manually curated using the information
551 provided in the respective publications or by contacting the original authors/submitters.
552 Annotare [51] was used for annotating the metadata and stored using the Investigation
553 Description Format (IDF) and Sample-Data Relationship Format (SDRF) file formats [42],
554 which are required for integration in Expression Atlas. An overview of the experimental
555 design including experimental factors, protocols, publication information and contact

556 information are present in the IDF file, and the SDRF includes sample metadata describing
557 the relationship between the various sample characteristics and the data files contained in the
558 dataset.
559
560 **4.2. Proteomics raw data processing**
561 All datasets were analysed with MaxQuant (version 1.6.3.4) [52, 53] on a Linux high-
562 performance computing cluster for peptide/protein identification and protein quantification.
563 Input parameters for each dataset, such as MS^1 and MS^2 tolerances, digesting enzymes, fixed
564 and variable modifications, were set as described in their respective publications, with two
565 missed cleavage sites. The FDR at the PSM (peptide spectrum match) and protein levels were
566 set to 1%. The MaxQuant parameters were otherwise set to default values: the maximum
567 number of modifications per peptide was 5, the minimum peptide length was 7, the maximum
568 peptide mass was set to 4,600 Da, and for the matches between runs the minimum match time
569 window was set to 0.7 seconds and the minimum retention time alignment window was set to
570 20 seconds. The MaxQuant parameter files are available for downloading from Expression
571 Atlas. The *Mus musculus* UniProt Reference proteome release-2021_04 (including isoforms,
572 63,656 sequences) and *Rattus norvegicus* UniProt Reference proteome release-2021_04
573 (including isoforms, 31,562 sequences) were used as the target sequence databases for mouse
574 and rat datasets, respectively. The built-in contaminant database within MaxQuant was used
575 and a decoy database was generated by MaxQuant by reversing the input database sequences
576 after the respective enzymatic digestion. The datasets were run separately in multi-threaded
577 mode.
578
579 **4.3. Post-processing**

580 The post-processing of results from MaxQuant is explained in detail in [14]. In brief, the
581 protein groups labelled as potential contaminants, decoys and those with fewer than 2 PSMs
582 were removed. Protein intensities in each sample were normalised by scaling the iBAQ
583 intensity values to the total amount of signal in each MS run and converted to parts per
584 billion (ppb).

585 $$ppb_iBAQ_i = \left({iBAQ_i}/{\sum_{i=1}^{n} iBAQ_i} \right) x\ 1{,}000{,}000{,}000$$

586 The 'majority protein identifiers' within each protein group were mapped to their Ensembl
587 gene identifiers/annotations using the Bioconductor package 'mygene'. For downstream
588 analysis only protein groups whose isoforms mapped to a single unique Ensembl gene ID
589 were considered. Protein groups that mapped to more than one Ensembl gene ID are provided
590 in Supplementary File 1. The protein intensity values from different protein groups with the
591 same Ensembl gene ID were aggregated as median values. The parent genes to which the
592 different protein groups were mapped to are equivalent to 'canonical proteins' in UniProt
593 (https://www.uniprot.org/help/canonical_and_isoforms) and therefore the term protein
594 abundance is used to describe the protein abundance of the canonical protein throughout the
595 manuscript.
596

597 **4.4. Integration into Expression Atlas**

598 The calculated canonical protein abundances (mapped to genes), together with the validated
599 SDRF files, summary files detailing the quality of post-processing and the input MaxQuant
600 parameter files (mqpar.xml) were integrated into Expression Atlas
601 (https://www.ebi.ac.uk/gxa/home) as proteomics baseline experiments (E-PROT identifiers
602 are available in Table 1).
603

604 **4.5. Protein abundance comparison across datasets**

605 To compare protein abundances, the normalised protein abundances (in ppb) from each group
606 of tissues in a dataset were converted into ranked bins. In this study, 'tissue' is defined as a
607 distinct functional or structural region within an 'organ'. For example, hippocampus,
608 cerebellum and cortex are defined as 'tissues' that are part of the brain (organ) and similarly
609 sinus node, left atria, left ventricle, right atria, right ventricle are defined as 'tissues' in heart
610 (organ). Protein abundances were transformed into bins by first grouping MS runs from each
611 tissue within a dataset as a batch. The normalised protein abundances (ppb) for each MS run
612 within a batch were sorted from lowest to highest abundance and ranked into 5 bins. Proteins
613 whose ppb abundances are ranked in the lowest bin (bin 1) represent lowest abundance and
614 correspondingly proteins within bin 5 are of highest abundance in their respective tissue.
615 When merging tissues into organs, median bin values were used.

616 Proteins that were detected in at least 50% of the samples were selected for PCA (Principal
617 Component Analysis) and was performed using R (The R Stats package) [54] using binned
618 abundance values. For generating heatmaps, a Pearson correlation coefficient for all samples
619 was calculated on pairwise complete observations of bin transformed values. Missing values
620 were marked as NA (not available). For each organ a median R^2 was calculated from all
621 pairwise R^2 values of their respective samples. Samples were hierarchically clustered on
622 columns and rows using Euclidean distances. To compare the correlation in protein
623 expression of shared organs between datasets, the FOT normalised protein abundances (ppb)
624 were aggregated by calculating the median over samples. The regression line was computed
625 using the 'linear model' (lm) method in R.

626 **4.6 Comparison of protein abundances using iBAQ and spectral counting data available**
627 **in PaxDB**

628 To compare protein abundances generated from iBAQ in this study and spectral counting
629 methods, protein abundance data from different mouse organs was obtained from PaxDB
630 (https://www.pax-db.org/) [16]. FOT normalised iBAQ abundances, as described above, were
631 compared with the spectral counting abundances for the matching mouse organs. Organs
632 from mouse labelled as 'integrated' in PaxDB were selected. It was not possible to perform
633 this comparison for rat organs since data in PaxDB for rat are available for either the 'whole
634 organism' or for "cell types" only. Abundances were compared across mouse adipose tissue,
635 brain, heart, kidney, liver, lung, pancreas and spleen. The Ensembl ENSG gene ids were
636 mapped to ENSP protein ids in PaxDB using the 'mygene' bioconductor package in R.

637 **4.7. UMAP analysis**

638 To generate the UMAP visualisations we used the binned protein abundance values generated
639 in this study from rat and mouse, as well as the binned human protein abundance values from
640 [14]. First, we reduced this data to only contain the orthologs found in all three species. For
641 the purpose of only the initial visualisation layout, we filtered the data to include those
642 proteins present in 90% of samples. Once the initial layout was generated, we then used the
643 full protein abundance values to generate protein-specific visualisations. We use R v4.1.0
644 with the package 'umap' (Uniform Manifold Approximation and Projection in R) [55]
645 v0.2.7.0 to generate the UMAP visualisations.

646 **4.8. Organ-specific expression profile analysis**

647 For comparison across organs, the tissues were aggregated into organs and their median bin
648 values were considered. As described previously [14] the classification scheme done by
649 Uhlén *et al.* [17] was modified to classify the proteins into one of the three categories: (1)
650 "Organ-enriched": present in one unique organ with bin values 2-fold higher than the mean

651 bin value across all organs; (2) “Group enriched”: present in at least 7 organs in mouse or in
652 at least 4 organs in rat, with bin values 2-fold higher than the mean bin value across all
653 organs; and (3) “Mixed”: the remaining canonical proteins that are not part of the above two
654 categories.
655
656 Enriched gene ontology (GO) terms analysis was carried out through over-representation test
657 described previously [14], it was combined with “Organ-enriched” and “Group enriched”
658 mapped gene lists for each organ. In addition, Reactome [56] pathway analysis was
659 performed using mapped gene lists and running pathway-topology and over-representation
660 analysis, as reported previously [14].

661 **4.9. Comparison of protein expression across species**

662 The g:Orth Orthology search function in the g:Profiler suite of programs [57] was used for
663 translating gene identifiers between organisms. Since a custom list of gene identifiers could
664 not be used as the background search set, the mouse and rat genes were first mapped against
665 the background Ensembl database. The resulting list of mouse and rat genes mapped to
666 human orthologs were then filtered so that they only included parent gene identifiers of the
667 protein groups from mouse and rat organs identified in this study and the parent genes of
668 human organs described in our previous study (Supplementary File 2 in [14]), respectively.
669
670 The orthologs were grouped into various categories denoting the resulting mapping between
671 identifiers: “one-to-one”, “one-to-many”, “many-to-one”, “many-to-many”, and “no
672 mappings” between gene identifiers. Only “one-to-one” mapped ortholog identifiers were
673 used to compare protein intensities between mouse, rat and human organs. The normalised
674 ppb protein abundances of the one-to-one mapped orthologues in 6 organs (brain, heart,

kidney, liver, lung and testis), that were studied across all three organisms were used to assess the pairwise correlation of protein abundances. The linear regression was calculated using the linear fit 'lm' method in R.

Data availability

Expression Atlas E-PROT identifiers and PRIDE original dataset identifiers are included in Table 1.

Acknowledgements

First of all, we would like to thank all data submitters who made their datasets available via PRIDE and ProteomeXchange. We would also like to thank Andrew Leach and the rest of the team involved in the Open Targets "Target Safety" project, for helpful discussions.

Authors' contributions

SW, DGS, AP, DJK selected and curated the datasets. SW, AP, DGS performed analyses. AC and ARJ helped in the interpretation of results and designed approach for data normalisation. NG, SF, PM, and IP helped in the integration of the results into Expression Atlas. SW, AP, DGS, JAV wrote the manuscript. JAV, ARJ and IP obtained the funding for performing the study. All authors have read and approved the manuscript.

Funding

AP and DGS were funded by Open Targets (project OTAR-02-068), https://www.opentargets.org/. AP, IP, NG, PM, SF and JAV were funded by BBSRC BB/T019670/1, https://bbsrc.ukri.org/. AC and ARJ were funded by BBSRC BB/T019557/1, https://bbsrc.ukri.org/. AP, DGS, SW and JAV were funded by Wellcome Trust [grant

number 208391/Z/17/Z], https://wellcome.org/. DJK, IP and JAV were funded by EMBL core funding, https://www.embl.org/. The funders had no role in study design, data collection and analysis, decision to publish, or preparation of the manuscript.

Supporting information

Supplementary file 1: Protein groups from all datasets that are mapped to more than one Ensembl Gene ID.

Supplementary file 2: Median protein abundances (in ppb) for each protein group across various tissue samples in each organ.

Supplementary file 3: Median binned protein abundances across various tissue samples in each organ of mouse and rat.

Supplementary file 4: Supplementary figures (S1) illustrating correlation of protein abundances in organs represented in different datasets. (S2) Correlation of protein abundances generated using iBAQ and spectral counting methods in various mouse organs. (S3) Correlation of protein expression between organs within human, mouse and rat.

Supplementary file 5: Organ distribution of canonical proteins in mouse and rat.

Supplementary file 6: Gene Ontology enrichment analysis of 'organ-enriched' and 'group-enriched' proteins.

Supplementary file 7: Binned protein abundances of one-to-one mapped orthologs across all organs studied.

Supplementary file 8: Figure illustrating binned protein abundances of all one-to-one mapped orthologs across six common organs in mouse, rat and human.

Supplementary file 9: UMAP co-ordinates and source data of UMAP analysis.

721

722 **Abbreviations**

723 DDA: Data Dependent Acquisition

724 DIA: Data Independent Acquisition

725 FOT: Fraction of Total

726 GO: Gene Ontology

727 iBAQ: intensity-based absolute quantification

728 iTRAQ: Isobaric tag for relative and absolute quantitation

729 IDF: Investigation Description Format

730 MS: Mass Spectrometry

731 ppb: Parts per billion

732 PCA: Principal Component Analysis

733 SDRF: Sample and Data Relationship Format

734 TMT: Tandem Mass Tagging

735 UMAP: Uniform Manifold Approximation and Projection

736 **References**
737
738 1. Aebersold R, Mann M. Mass-spectrometric exploration of proteome structure and
739 function. Nature. 2016;537(7620):347-55. Epub 2016/09/16. doi: 10.1038/nature19949.
740 PubMed PMID: 27629641.
741 2. Perez-Riverol Y, Csordas A, Bai J, Bernal-Llinares M, Hewapathirana S, Kundu DJ,
742 et al. The PRIDE database and related tools and resources in 2019: improving support for
743 quantification data. Nucleic Acids Res. 2019;47(D1):D442-D50. Epub 2018/11/06. doi:
744 10.1093/nar/gky1106. PubMed PMID: 30395289; PubMed Central PMCID:
745 PMCPMC6323896.
746 3. Vizcaino JA, Deutsch EW, Wang R, Csordas A, Reisinger F, Rios D, et al.
747 ProteomeXchange provides globally coordinated proteomics data submission and
748 dissemination. Nat Biotechnol. 2014;32(3):223-6. Epub 2014/04/15. doi: 10.1038/nbt.2839.
749 PubMed PMID: 24727771; PubMed Central PMCID: PMCPMC3986813.
750 4. Martens L, Vizcaino JA. A Golden Age for Working with Public Proteomics Data.
751 Trends Biochem Sci. 2017;42(5):333-41. Epub 2017/01/26. doi: 10.1016/j.tibs.2017.01.001.
752 PubMed PMID: 28118949; PubMed Central PMCID: PMCPMC5414595.
753 5. Romanov N, Kuhn M, Aebersold R, Ori A, Beck M, Bork P. Disentangling Genetic
754 and Environmental Effects on the Proteotypes of Individuals. Cell. 2019;177(5):1308-18 e10.
755 Epub 2019/04/30. doi: 10.1016/j.cell.2019.03.015. PubMed PMID: 31031010; PubMed
756 Central PMCID: PMCPMC6988111.
757 6. Skinnider MA, Foster LJ. Meta-analysis defines principles for the design and analysis
758 of co-fractionation mass spectrometry experiments. Nat Methods. 2021;18(7):806-15. Epub
759 2021/07/03. doi: 10.1038/s41592-021-01194-4. PubMed PMID: 34211188.
760 7. Ochoa D, Jarnuczak AF, Vieitez C, Gehre M, Soucheray M, Mateus A, et al. The
761 functional landscape of the human phosphoproteome. Nat Biotechnol. 2020;38(3):365-73.
762 Epub 2019/12/11. doi: 10.1038/s41587-019-0344-3. PubMed PMID: 31819260; PubMed
763 Central PMCID: PMCPMC7100915.
764 8. Vaudel M, Verheggen K, Csordas A, Raeder H, Berven FS, Martens L, et al.
765 Exploring the potential of public proteomics data. Proteomics. 2016;16(2):214-25. Epub
766 2015/10/10. doi: 10.1002/pmic.201500295. PubMed PMID: 26449181; PubMed Central
767 PMCID: PMCPMC4738454.
768 9. Kumar D, Yadav AK, Jia X, Mulvenna J, Dash D. Integrated Transcriptomic-
769 Proteomic Analysis Using a Proteogenomic Workflow Refines Rat Genome Annotation. Mol
770 Cell Proteomics. 2016;15(1):329-39. Epub 2015/11/13. doi: 10.1074/mcp.M114.047126.
771 PubMed PMID: 26560066; PubMed Central PMCID: PMCPMC4762527.
772 10. Brunet MA, Brunelle M, Lucier JF, Delcourt V, Levesque M, Grenier F, et al.
773 OpenProt: a more comprehensive guide to explore eukaryotic coding potential and
774 proteomes. Nucleic Acids Res. 2019;47(D1):D403-D10. Epub 2018/10/10. doi:
775 10.1093/nar/gky936. PubMed PMID: 30299502; PubMed Central PMCID:
776 PMCPMC6323990.
777 11. Levitsky LI, Kliuchnikova AA, Kuznetsova KG, Karpov DS, Ivanov MV, Pyatnitskiy
778 MA, et al. Adenosine-to-Inosine RNA Editing in Mouse and Human Brain Proteomes.
779 Proteomics. 2019;19(23):e1900195. Epub 2019/10/03. doi: 10.1002/pmic.201900195.
780 PubMed PMID: 31576663.
781 12. Li H, Zhou R, Xu S, Chen X, Hong Y, Lu Q, et al. Improving Gene Annotation of the
782 Peanut Genome by Integrated Proteogenomics Workflow. J Proteome Res. 2020;19(6):2226-
783 35. Epub 2020/05/06. doi: 10.1021/acs.jproteome.9b00723. PubMed PMID: 32367721.
784 13. Jarnuczak AF, Najgebauer H, Barzine M, Kundu DJ, Ghavidel F, Perez-Riverol Y, et
785 al. An integrated landscape of protein expression in human cancer. Sci Data. 2021;8(1):115.

786 Epub 2021/04/25. doi: 10.1038/s41597-021-00890-2. PubMed PMID: 33893311; PubMed
787 Central PMCID: PMCPMC8065022.
788 14. Prakash A, García-Seisdedos D, Wang S, Kundu DJ, Collins A, George N, et al. An
789 integrated view of baseline protein expression in human tissues. bioRxiv.
790 2021:2021.09.10.459811. doi: 10.1101/2021.09.10.459811.
791 15. Samaras P, Schmidt T, Frejno M, Gessulat S, Reinecke M, Jarzab A, et al.
792 ProteomicsDB: a multi-omics and multi-organism resource for life science research. Nucleic
793 Acids Res. 2020;48(D1):D1153-D63. Epub 2019/10/31. doi: 10.1093/nar/gkz974. PubMed
794 PMID: 31665479; PubMed Central PMCID: PMCPMC7145565.
795 16. Wang M, Herrmann CJ, Simonovic M, Szklarczyk D, von Mering C. Version 4.0 of
796 PaxDb: Protein abundance data, integrated across model organisms, tissues, and cell-lines.
797 Proteomics. 2015;15(18):3163-8. Epub 2015/02/07. doi: 10.1002/pmic.201400441. PubMed
798 PMID: 25656970; PubMed Central PMCID: PMCPMC6680238.
799 17. Uhlen M, Fagerberg L, Hallstrom BM, Lindskog C, Oksvold P, Mardinoglu A, et al.
800 Proteomics. Tissue-based map of the human proteome. Science. 2015;347(6220):1260419.
801 Epub 2015/01/24. doi: 10.1126/science.1260419. PubMed PMID: 25613900.
802 18. Azimifar SB, Nagaraj N, Cox J, Mann M. Cell-type-resolved quantitative proteomics
803 of murine liver. Cell Metab. 2014;20(6):1076-87. Epub 2014/12/04. doi:
804 10.1016/j.cmet.2014.11.002. PubMed PMID: 25470552.
805 19. Deshmukh AS, Murgia M, Nagaraj N, Treebak JT, Cox J, Mann M. Deep proteomics
806 of mouse skeletal muscle enables quantitation of protein isoforms, metabolic pathways, and
807 transcription factors. Mol Cell Proteomics. 2015;14(4):841-53. Epub 2015/01/27. doi:
808 10.1074/mcp.M114.044222. PubMed PMID: 25616865; PubMed Central PMCID:
809 PMCPMC4390264.
810 20. Meierhofer D, Halbach M, Sen NE, Gispert S, Auburger G. Ataxin-2 (Atxn2)-Knock-
811 Out Mice Show Branched Chain Amino Acids and Fatty Acids Pathway Alterations. Mol
812 Cell Proteomics. 2016;15(5):1728-39. Epub 2016/02/07. doi: 10.1074/mcp.M115.056770.
813 PubMed PMID: 26850065; PubMed Central PMCID: PMCPMC4858951.
814 21. Sarver DC, Kharaz YA, Sugg KB, Gumucio JP, Comerford E, Mendias CL. Sex
815 differences in tendon structure and function. J Orthop Res. 2017;35(10):2117-26. Epub
816 2017/01/11. doi: 10.1002/jor.23516. PubMed PMID: 28071813; PubMed Central PMCID:
817 PMCPMC5503813.
818 22. Duda P, Wojcicka O, Wisniewski JR, Rakus D. Global quantitative TPA-based
819 proteomics of mouse brain structures reveals significant alterations in expression of proteins
820 involved in neuronal plasticity during aging. Aging (Albany NY). 2018;10(7):1682-97. Epub
821 2018/07/22. doi: 10.18632/aging.101501. PubMed PMID: 30026405; PubMed Central
822 PMCID: PMCPMC6075443.
823 23. Harman JC, Guidry JJ, Gidday JM. Comprehensive characterization of the adult ND4
824 Swiss Webster mouse retina: Using discovery-based mass spectrometry to decipher the total
825 proteome and phosphoproteome. Mol Vis. 2018;24:875-89. Epub 2019/02/05. PubMed
826 PMID: 30713425; PubMed Central PMCID: PMCPMC6334985.
827 24. Angelidis I, Simon LM, Fernandez IE, Strunz M, Mayr CH, Greiffo FR, et al. An
828 atlas of the aging lung mapped by single cell transcriptomics and deep tissue proteomics. Nat
829 Commun. 2019;10(1):963. Epub 2019/03/01. doi: 10.1038/s41467-019-08831-9. PubMed
830 PMID: 30814501; PubMed Central PMCID: PMCPMC6393476.
831 25. Zhao Y, Wilmarth PA, Cheng C, Limi S, Fowler VM, Zheng D, et al. Proteome-
832 transcriptome analysis and proteome remodeling in mouse lens epithelium and fibers. Exp
833 Eye Res. 2019;179:32-46. Epub 2018/10/26. doi: 10.1016/j.exer.2018.10.011. PubMed
834 PMID: 30359574; PubMed Central PMCID: PMCPMC6360118.

26. Huttlin EL, Jedrychowski MP, Elias JE, Goswami T, Rad R, Beausoleil SA, et al. A tissue-specific atlas of mouse protein phosphorylation and expression. Cell. 2010;143(7):1174-89. Epub 2010/12/25. doi: 10.1016/j.cell.2010.12.001. PubMed PMID: 21183079.
27. Linscheid N, Santos A, Poulsen PC, Mills RW, Calloe K, Leurs U, et al. Quantitative proteome comparison of human hearts with those of model organisms. PLoS Biol. 2021;19(4):e3001144. Epub 2021/04/20. doi: 10.1371/journal.pbio.3001144. PubMed PMID: 33872299; PubMed Central PMCID: PMCPMC8084454.
28. Dudek M, Angelucci C, Pathiranage D, Wang P, Mallikarjun V, Lawless C, et al. Circadian time series proteomics reveals daily dynamics in cartilage physiology. Osteoarthritis Cartilage. 2021;29(5):739-49. Epub 2021/02/22. doi: 10.1016/j.joca.2021.02.008. PubMed PMID: 33610821; PubMed Central PMCID: PMCPMC8113022.
29. Schroeder S, Hofer SJ, Zimmermann A, Pechlaner R, Dammbrueck C, Pendl T, et al. Dietary spermidine improves cognitive function. Cell Rep. 2021;35(2):108985. Epub 2021/04/15. doi: 10.1016/j.celrep.2021.108985. PubMed PMID: 33852843.
30. Bundy JL, Vied C, Nowakowski RS. Sex differences in the molecular signature of the developing mouse hippocampus. BMC Genomics. 2017;18(1):237. Epub 2017/03/18. doi: 10.1186/s12864-017-3608-7. PubMed PMID: 28302071; PubMed Central PMCID: PMCPMC5356301.
31. Linscheid N, Logantha S, Poulsen PC, Zhang S, Schrolkamp M, Egerod KL, et al. Quantitative proteomics and single-nucleus transcriptomics of the sinus node elucidates the foundation of cardiac pacemaking. Nat Commun. 2019;10(1):2889. Epub 2019/06/30. doi: 10.1038/s41467-019-10709-9. PubMed PMID: 31253831; PubMed Central PMCID: PMCPMC6599035.
32. Alugubelly N, Mohammed AN, Edelmann MJ, Nanduri B, Sayed M, Park JW, et al. Adolescent rat social play: Amygdalar proteomic and transcriptomic data. Data Brief. 2019;27:104589. Epub 2019/11/02. doi: 10.1016/j.dib.2019.104589. PubMed PMID: 31673590; PubMed Central PMCID: PMCPMC6817652.
33. Roffia V, De Palma A, Lonati C, Di Silvestre D, Rossi R, Mantero M, et al. Proteome Investigation of Rat Lungs subjected to Ex Vivo Perfusion (EVLP). Molecules. 2018;23(12). Epub 2018/11/24. doi: 10.3390/molecules23123061. PubMed PMID: 30467300; PubMed Central PMCID: PMCPMC6321151.
34. Bernier M, Harney D, Koay YC, Diaz A, Singh A, Wahl D, et al. Elucidating the mechanisms by which disulfiram protects against obesity and metabolic syndrome. NPJ Aging Mech Dis. 2020;6:8. Epub 2020/07/28. doi: 10.1038/s41514-020-0046-6. PubMed PMID: 32714562; PubMed Central PMCID: PMCPMC7374720.
35. Huang Q, Luo L, Alamdar A, Zhang J, Liu L, Tian M, et al. Integrated proteomics and metabolomics analysis of rat testis: Mechanism of arsenic-induced male reproductive toxicity. Sci Rep. 2016;6:32518. Epub 2016/09/03. doi: 10.1038/srep32518. PubMed PMID: 27585557; PubMed Central PMCID: PMCPMC5009432.
36. Kaushik G, Spenlehauer A, Sessions AO, Trujillo AS, Fuhrmann A, Fu Z, et al. Vinculin network-mediated cytoskeletal remodeling regulates contractile function in the aging heart. Sci Transl Med. 2015;7(292):292ra99. Epub 2015/06/19. doi: 10.1126/scitranslmed.aaa5843. PubMed PMID: 26084806; PubMed Central PMCID: PMCPMC4507505.
37. Vileigas DF, Harman VM, Freire PP, Marciano CLC, Sant'Ana PG, de Souza SLB, et al. Landscape of heart proteome changes in a diet-induced obesity model. Sci Rep. 2019;9(1):18050. Epub 2019/12/04. doi: 10.1038/s41598-019-54522-2. PubMed PMID: 31792287; PubMed Central PMCID: PMCPMC6888820.

885 38. Limbutara K, Chou CL, Knepper MA. Quantitative Proteomics of All 14 Renal
886 Tubule Segments in Rat. J Am Soc Nephrol. 2020;31(6):1255-66. Epub 2020/05/03. doi:
887 10.1681/ASN.2020010071. PubMed PMID: 32358040; PubMed Central PMCID:
888 PMCPMC7269347.
889 39. Devaux S, Cizkova D, Quanico J, Franck J, Nataf S, Pays L, et al. Proteomic Analysis
890 of the Spatio-temporal Based Molecular Kinetics of Acute Spinal Cord Injury Identifies a
891 Time- and Segment-specific Window for Effective Tissue Repair. Mol Cell Proteomics.
892 2016;15(8):2641-70. Epub 2016/06/03. doi: 10.1074/mcp.M115.057794. PubMed PMID:
893 27250205; PubMed Central PMCID: PMCPMC4974342.
894 40. Choi H, Simpson D, Wang D, Prescott M, Pitsillides AA, Dudhia J, et al.
895 Heterogeneity of proteome dynamics between connective tissue phases of adult tendon. Elife.
896 2020;9. Epub 2020/05/13. doi: 10.7554/eLife.55262. PubMed PMID: 32393437; PubMed
897 Central PMCID: PMCPMC7217697.
898 41. Hodge K, Have ST, Hutton L, Lamond AI. Cleaning up the masses: exclusion lists to
899 reduce contamination with HPLC-MS/MS. J Proteomics. 2013;88:92-103. Epub 2013/03/19.
900 doi: 10.1016/j.jprot.2013.02.023. PubMed PMID: 23501838; PubMed Central PMCID:
901 PMCPMC3714598.
902 42. Dai C, Fullgrabe A, Pfeuffer J, Solovyeva EM, Deng J, Moreno P, et al. A proteomics
903 sample metadata representation for multiomics integration and big data analysis. Nat
904 Commun. 2021;12(1):5854. Epub 2021/10/08. doi: 10.1038/s41467-021-26111-3. PubMed
905 PMID: 34615866; PubMed Central PMCID: PMCPMC8494749.
906 43. Evans R, O'Neill M, Pritzel A, Antropova N, Senior A, Green T, et al. Protein
907 complex prediction with AlphaFold-Multimer. bioRxiv. 2021:2021.10.04.463034. doi:
908 10.1101/2021.10.04.463034.
909 44. Bregman CL, Adler RR, Morton DG, Regan KS, Yano BL, Society of Toxicologic P.
910 Recommended tissue list for histopathologic examination in repeat-dose toxicity and
911 carcinogenicity studies: a proposal of the Society of Toxicologic Pathology (STP). Toxicol
912 Pathol. 2003;31(2):252-3. Epub 2003/04/17. doi: 10.1080/01926230390183751. PubMed
913 PMID: 12696587.
914 45. Walzer M, García-Seisdedos D, Prakash A, Brack P, Crowther P, Graham RL, et al.
915 Implementing the re-use of public DIA proteomics datasets: from the PRIDE database to
916 Expression Atlas. bioRxiv. 2021:2021.06.08.447493. doi: 10.1101/2021.06.08.447493.
917 46. Sollner JF, Leparc G, Hildebrandt T, Klein H, Thomas L, Stupka E, et al. An RNA-
918 Seq atlas of gene expression in mouse and rat normal tissues. Sci Data. 2017;4:170185. Epub
919 2017/12/13. doi: 10.1038/sdata.2017.185. PubMed PMID: 29231921; PubMed Central
920 PMCID: PMCPMC5726313.
921 47. Sudmant PH, Alexis MS, Burge CB. Meta-analysis of RNA-seq expression data
922 across species, tissues and studies. Genome Biol. 2015;16:287. Epub 2015/12/24. doi:
923 10.1186/s13059-015-0853-4. PubMed PMID: 26694591; PubMed Central PMCID:
924 PMCPMC4699362.
925 48. Zheng-Bradley X, Rung J, Parkinson H, Brazma A. Large scale comparison of global
926 gene expression patterns in human and mouse. Genome Biol. 2010;11(12):R124. Epub
927 2010/12/25. doi: 10.1186/gb-2010-11-12-r124. PubMed PMID: 21182765; PubMed Central
928 PMCID: PMCPMC3046484.
929 49. Liao BY, Zhang J. Evolutionary conservation of expression profiles between human
930 and mouse orthologous genes. Mol Biol Evol. 2006;23(3):530-40. Epub 2005/11/11. doi:
931 10.1093/molbev/msj054. PubMed PMID: 16280543.
932 50. Prasad A, Kumar SS, Dessimoz C, Bleuler S, Laule O, Hruz T, et al. Global
933 regulatory architecture of human, mouse and rat tissue transcriptomes. BMC Genomics.

2013;14:716. Epub 2013/10/22. doi: 10.1186/1471-2164-14-716. PubMed PMID: 24138449; PubMed Central PMCID: PMCPMC4008137.
51. Athar A, Fullgrabe A, George N, Iqbal H, Huerta L, Ali A, et al. ArrayExpress update - from bulk to single-cell expression data. Nucleic Acids Res. 2019;47(D1):D711-D5. Epub 2018/10/26. doi: 10.1093/nar/gky964. PubMed PMID: 30357387; PubMed Central PMCID: PMCPMC6323929.
52. Cox J, Mann M. MaxQuant enables high peptide identification rates, individualized p.p.b.-range mass accuracies and proteome-wide protein quantification. Nat Biotechnol. 2008;26(12):1367-72. Epub 2008/11/26. doi: 10.1038/nbt.1511. PubMed PMID: 19029910.
53. Tyanova S, Temu T, Cox J. The MaxQuant computational platform for mass spectrometry-based shotgun proteomics. Nat Protoc. 2016;11(12):2301-19. Epub 2016/11/04. doi: 10.1038/nprot.2016.136. PubMed PMID: 27809316.
54. Team RC. R: A language and environment for statistical computing. R Foundation for Statistical Computing, Vienna, Austria. ISBN 3-900051-07-0, URL http://www.R-project.org/. 2013.
55. McInnes L HJ, Melville J. UMAP: Uniform Manifold Approximation and Projection for dimension reduction. arXiv. 2018.
56. Wu G, Haw R. Functional Interaction Network Construction and Analysis for Disease Discovery. Methods Mol Biol. 2017;1558:235-53. Epub 2017/02/06. doi: 10.1007/978-1-4939-6783-4_11. PubMed PMID: 28150241.
57. Raudvere U, Kolberg L, Kuzmin I, Arak T, Adler P, Peterson H, et al. g:Profiler: a web server for functional enrichment analysis and conversions of gene lists (2019 update). Nucleic Acids Res. 2019;47(W1):W191-W8. Epub 2019/05/09. doi: 10.1093/nar/gkz369. PubMed PMID: 31066453; PubMed Central PMCID: PMCPMC6602461.